Evolution of Aluminum Aminophenolate Complexes in the Ring-Opening Polymerization of ε-Caprolactone: Electronic and Amino-Chelating Effects

Prasanna Kumar Ganta,[a‡] Fei Huang,[a‡] Taoufik Ben Halima,[b] Rajiv Kamaraj,[a] Yu-Ting Chu,[ac] Hsi-Ching Tseng,[d] Shangwu Ding,[ac] Kuo-Hui Wu*,[e] Hsuan-Ying Chen*[acfg]

[a] *Department of Medicinal and Applied Chemistry, Drug Development and Value Creation Research Center, Kaohsiung Medical University, Kaohsiung, Taiwan, 80708, R.O.C.*
[b] *Department of Chemistry & Biomolecular Sciences, University of Ottawa, Ottawa, Canada*
[c] *Department of Chemistry, National Sun Yat-Sen University, Kaohsiung, Taiwan, 80424, R.O.C.*
[d] *College of Science Instrumentation Center, National Taiwan University, Taipei, Taiwan, 106319, R.O.C.*
[e] *Department of Chemistry, National Central University, Taoyuan, Taiwan, 32001, R.O.C.*
[f] *Department of Medical Research, Kaohsiung Medical University Hospital, Kaohsiung 80708, Taiwan, R.O.C.*
[g] *National Pingtung University of Science and Technology, Pingtung, Taiwan 91201, R.O.C*

Supporting Information

Table of Contents

Table S1. Kinetic study of CL polymerization with $\mathbf{O^{Me}_2}$**-Al**, $\mathbf{O^{Br}_2}$**-Al**, $\mathbf{ON^{OMe}}$**-Al**, $\mathbf{ON^{Br}}$**-Al**, $\mathbf{O^{Me}}$**-Al**, and $\mathbf{O^{Br}}$**-Al**[a]

Time	[**L-Al**], **L**=					
(min)	$\mathbf{O^{Me}_2}$	$\mathbf{O^{Br}_2}$	$\mathbf{ON^{OMe}}$	$\mathbf{ON^{Br}}$	$\mathbf{O^{OMe}}$	$\mathbf{O^{Br}}$
	PCL conversion[b]					
2					0.07	
3			0.15	0.16		
4					0.23	
5	0.30		0.34	0.33		0.08
6					0.40	
8	0.64		0.58		0.56	
10	0.79		0.70	0.65	0.67	0.23
12	0.87				0.75	
13	0.90			0.76		
15		0.18	0.86		0.85	
16				0.83		
18					0.90	
20		0.57				0.46
30		0.87				0.63
35						
40		0.95				0.72
50						0.8
70						0.90

$k_{obs}\times 10^{-3}$/ min^{-1} (error)	244.5 (48)	112.1 (50)	152.0 (3)	124.4 (1)	143.2 (35)	33.9 (4)
I.P/ min (error)	4 (1)	13 (1)	2 (1)	2 (1)	2 (1)	2 (1)
R^2	0.999	0.998	0.999	0.999	0.998	0.999

[a] General, the reaction was carried out in toluene with [CL] = 2.00 M at 25 °C.
[b] The data were determined from ^{1}H NMR analysis.

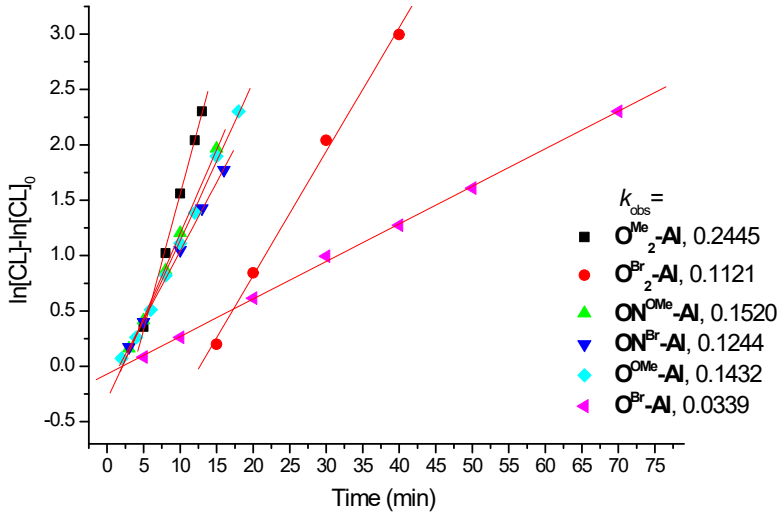

Figure S1. First-order kinetic plots of CL polymerization with various Al complexes (**O^{Me}_2-Al**, **O^{Br}_2-Al**, **ON^{OMe}-Al**, **ON^{Br}-Al**, **O^{Me}-Al**, and **O^{Br}-Al**) plotted against time with [CL] = 2.00 M in toluene 5.0 mL **(Table S1)**

Table S2. Kinetic study of CL polymerization with **NNO^{OMe}-Al**, **NNO^{Br}-Al**, **ONO^{OMe}-Al**, **ONO^{Br}-Al**, **$ONNO^{OMe}$-Al**, and **$ONNO^{Br}$-Al** [a]

Time	[L-Al], L=					
(min)	**NNO^{OMe}**	**NNO^{Br}**	**ONO^{OMe}**	**ONO^{Br}**	**$ONNO^{OMe}$**	**$ONNO^{Br}$**
	PCL conversion[b]					
5	0.26	0.14			0.05	0.06
10	0.44	0.30			0.35	

15	0.62				0.60	
20	0.73	0.54		0.08	0.76	0.46
25					0.85	
30	0.87	0.72		0.36	0.90	0.72
40	0.92	0.83				0.85
45			0.08			
50		0.88				0.91
55				0.78		
60		0.92	0.52	0.83		
65				0.87		
70			0.72			
75			0.78			
80			0.83			
$k_{obs}\times 10^{-3}$/ min^{-1} (error)	65.6 (23)	43.9 (1)	48.5 (1)	43.2 (1)	92.4 (2)	53.8 (2)
I.P/ min (error)	1 (1)	2 (2)	44 (2)	19 (2)	4 (1)	6 (2)
R^2	0.998	0.999	0.999	0.999	0.999	0.995

[a] General, the reaction was carried out in toluene with [CL] = 2.00 M at 25 °C.
[b] The data were determined from ^{1}H NMR analysis.

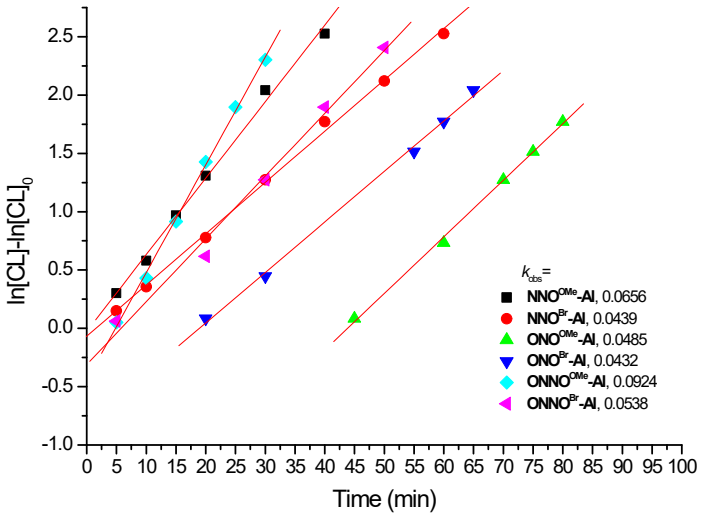

Figure S2. First-order kinetic plots of CL polymerization with various Al complexes (**NNO^{OMe}-Al**, **NNO^{Br}-Al**, **ONO^{OMe}-Al**, **ONO^{Br}-Al**, **ONNO^{OMe}-Al**, and **ONNO^{Br}-Al**) plotted against time with [CL] = 2.00 M in toluene 5.0 mL (**Table S1**).

Table S3. Kinetic study of CL polymerization with **NNOO^{OMe}-Al**, **NNOO^{Br}-Al**, **^{Bu}ONNO^{OMe}-Al**, **^{Bu}ONNO^{Br}-Al**, **OO^{OMe}-Al**, **OO^{Br}-Al**[a]

Time	[L-Al], L=					
(min)	**NNOO^{OMe}**	**NNOO^{Br}**	**^{Bu}ONNO^{OMe}**	**^{Bu}ONNO^{Br}**	**OO^{OMe}**	**OO^{Br}**
	PCL conversion[b]					
30	0.06					
60	0.20				0.10	
120	0.39			0.20	0.20	0.12
150	0.48					
180		0.24	0.15			
240		0.45		0.31	0.30	0.20
300	0.74		0.30			
420	0.86					
480					0.45	0.40

600					0.53	
840				0.70		
900		0.74			0.70	
960			0.78			
1020				0.77		
1080			0.82			0.64
1200				0.82		
1260		0.85				
1320			0.86	0.84		
1440			0.89			
1500			0.90			0.78
1560					0.90	
1620		0.92				
1680				0.90		
1920						0.85
2460						0.90
$k_{obs}\times 10^{-3}$/ min^{-1} (error)	4.83 (5)	1.46 (9)	1.62 (4)	1.35 (2)	1.44 (6)	0.95 (2)
I.P/ min (error)	16 (2)	0	66 (27)	0	14 (32)	0
R^2	0.999	0.994	0.998	0.999	0.995	0.999

[a] Generally, the reaction was carried out in toluene with [CL] = 2.00 M at 25 °C.

[b] The data were determined from ^{1}H NMR analysis.

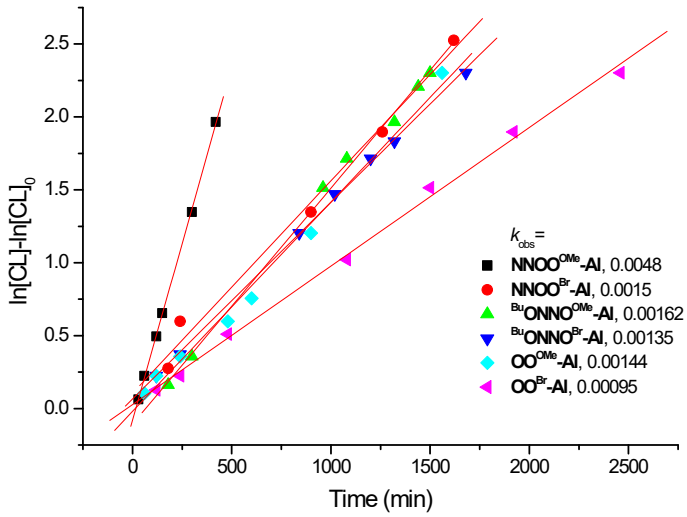

Figure S3. First-order kinetic plots of CL polymerization with various Al complexes (**NNOO^{OMe}-Al**, **NNOO^{Br}-Al**, **^{Bu}ONNO^{OMe}-Al**, **^{Bu}ONNO^{Br}-Al**, **OO^{OMe}-Al**, **OO^{Br}-Al**) plotted against time with [CL] = 2.00 M in toluene 5.0 mL (**Table S1**).

Table S4. Kinetic study of CL polymerization using **OO^{Bu}-Al** with BnOH and **(OO^{Bu}-AlOBn)$_2$** as catalysts, respectively, in toluene 5.0 mL, [CL] = 2.00 M at 25 °C [a].

	[CL]: [**OO^{Bu}-Al**]: [BnOH]=100:1:1	[CL]: **(OO^{Bu}-AlOBn)$_2$** = 100:0.5
Time (min)	PCL conversion (%) [b]	
60	10	
120	22	
180	37	9
240	57	
300	66	
360		18
420	79	
540	87	
660	93	
720		38
1020		52
1440		62

2460		85
2880		90
$k_{obs}\times 10^{-4}$/ min^{-1} (error)	43 (1)	8.0 (2)
I.P/ min (error)	53.32 (9.36)	129 (45)
R^2	0.99809	0.9961

[a] Generally, the reaction was carried out in toluene with [CL] = 2.00 M 25 °C.
[b] The data were determined from ^{1}H NMR analysis

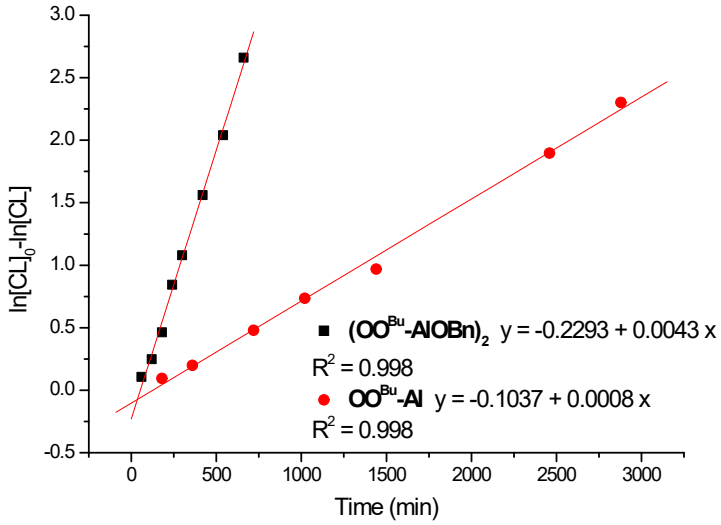

Figure S4. First-order kinetic plots of CL polymerization using **OO^{Bu}-Al** with BnOH and **(OO^{Bu}-AlOBn)$_2$** as catalysts, respectively, plotted against time with [CL] = 2.00 M in toluene 5.0 mL (**Table S4**)

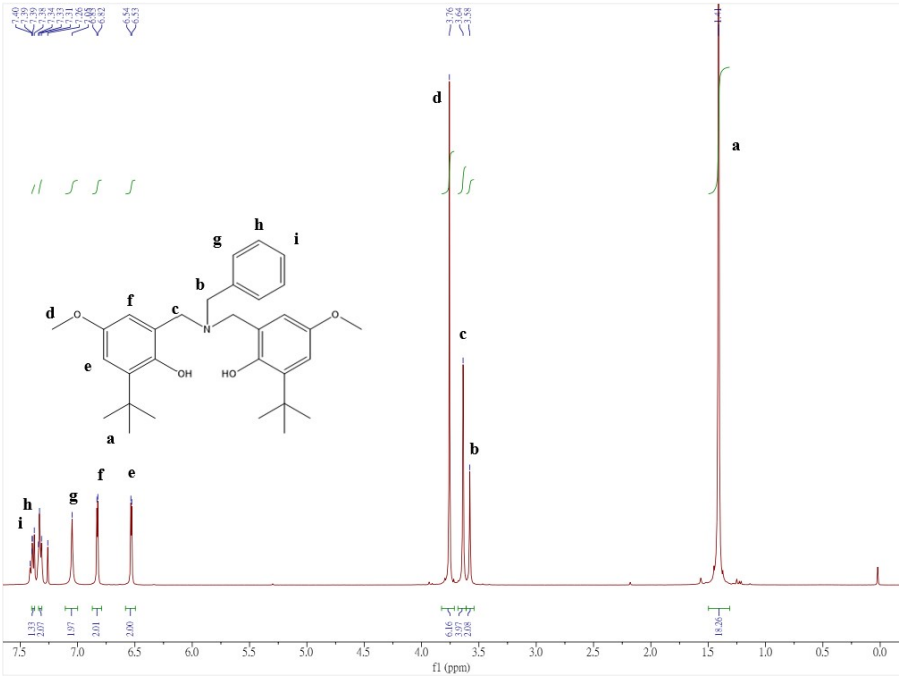

Figure S5. ^{1}H NMR spectrum of **ONO^{OMe}-H** in $CDCl_3$

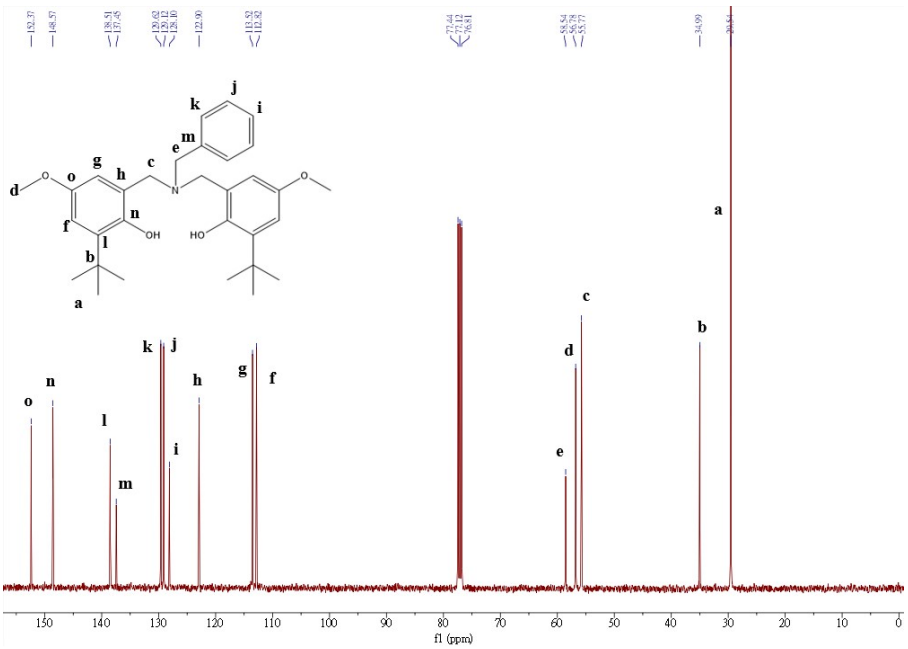

Figure S6. ^{13}C NMR spectrum of **ONO^{OMe}-H** in $CDCl_3$

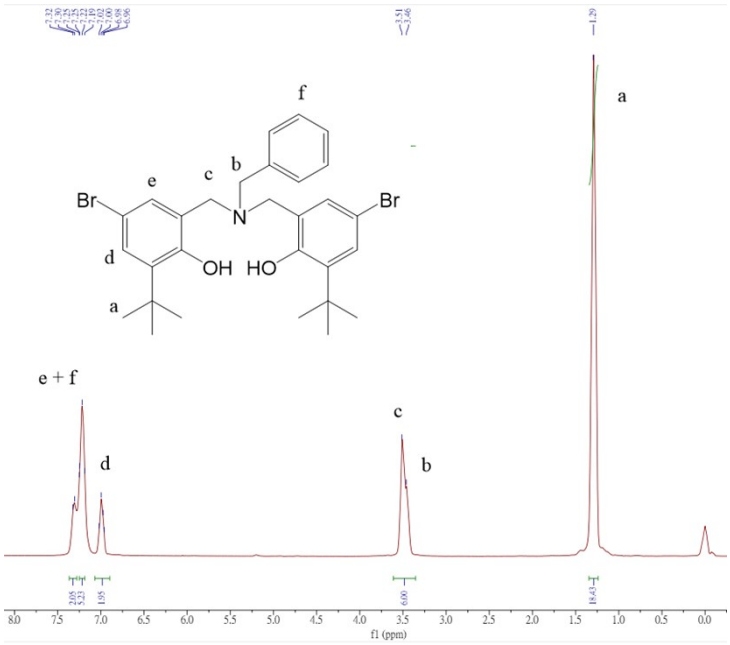

Figure S7. ^{1}H NMR spectrum of **ONO^{Br}-H** in $CDCl_3$

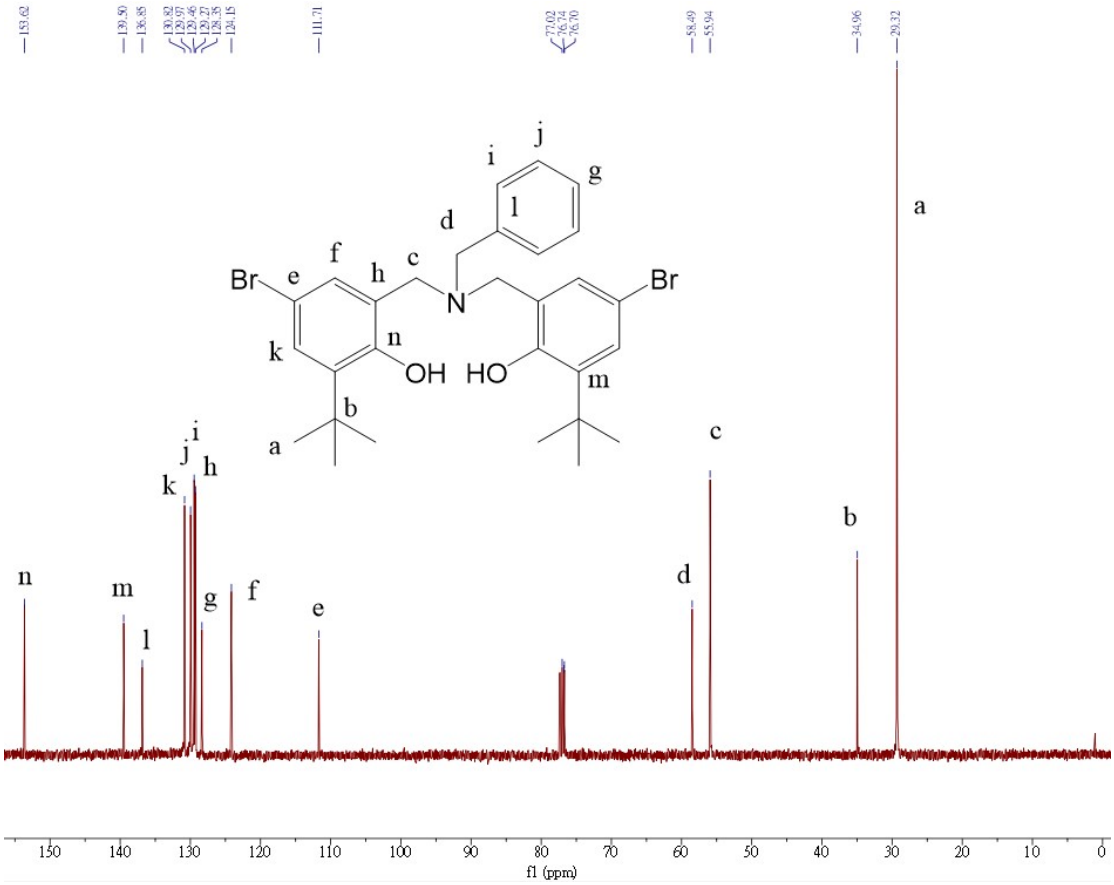

Figure S8. ^{13}C NMR spectrum of **ONO^{Br}-H** in $CDCl_3$

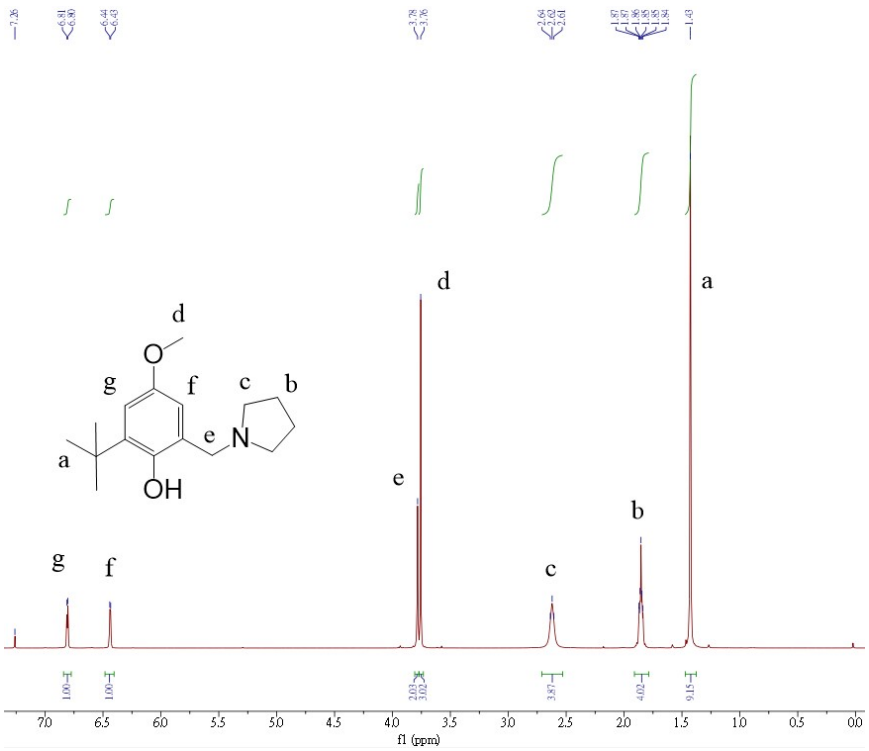

Figure S9. ^{1}H NMR spectrum of **ON^{OMe}-H** in $CDCl_3$

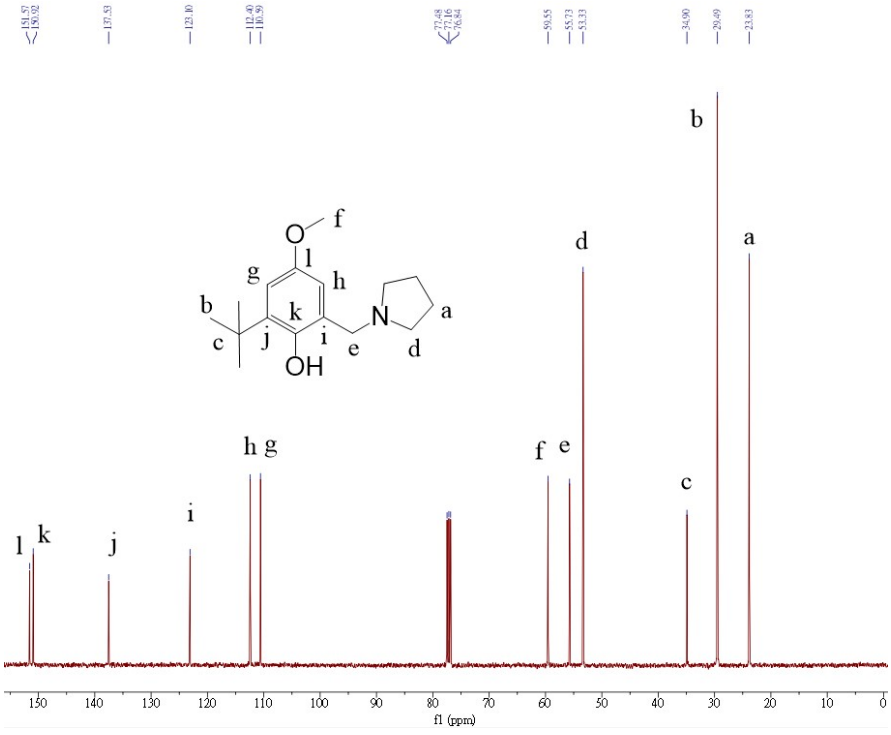

Figure S10. ^{13}C NMR spectrum of **ON^{OMe}-H** in $CDCl_3$

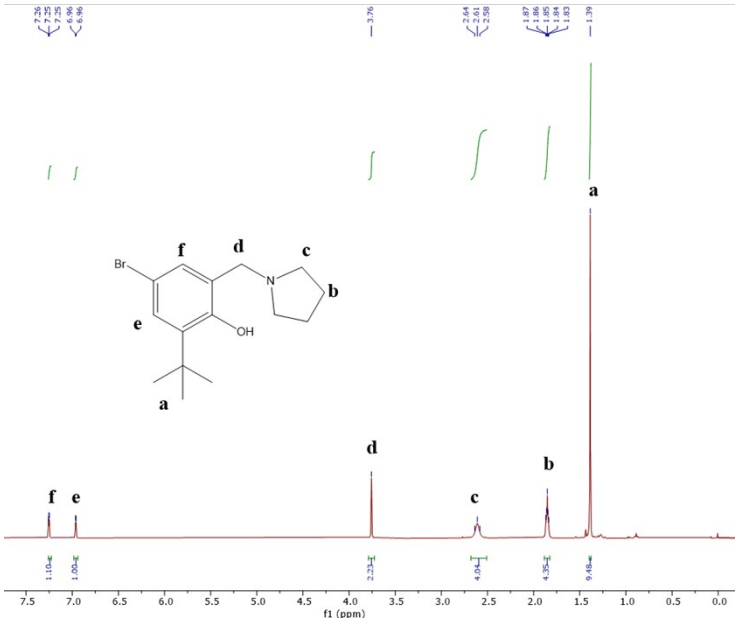

Figure S10. ^{1}H NMR spectrum of **ON^{Br}-H** in $CDCl_3$

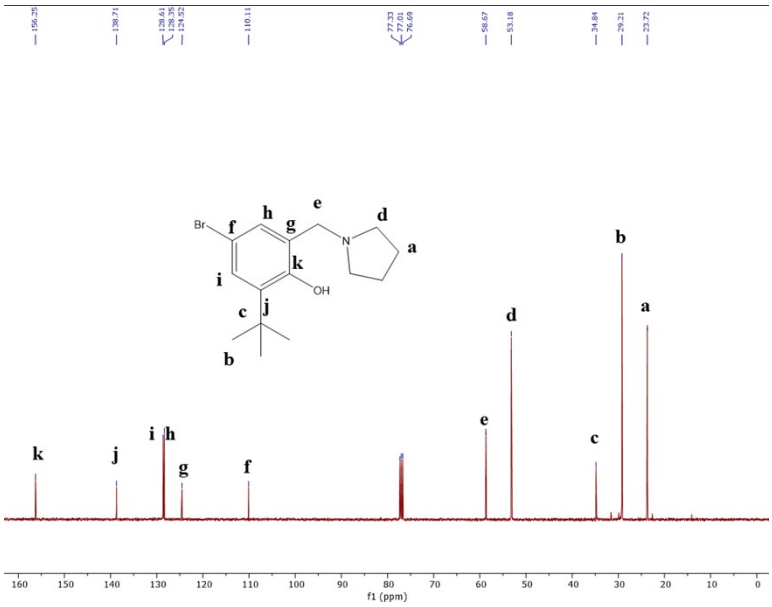

Figure S11. ^{13}C NMR spectrum of **ON^{Br}-H** in $CDCl_3$

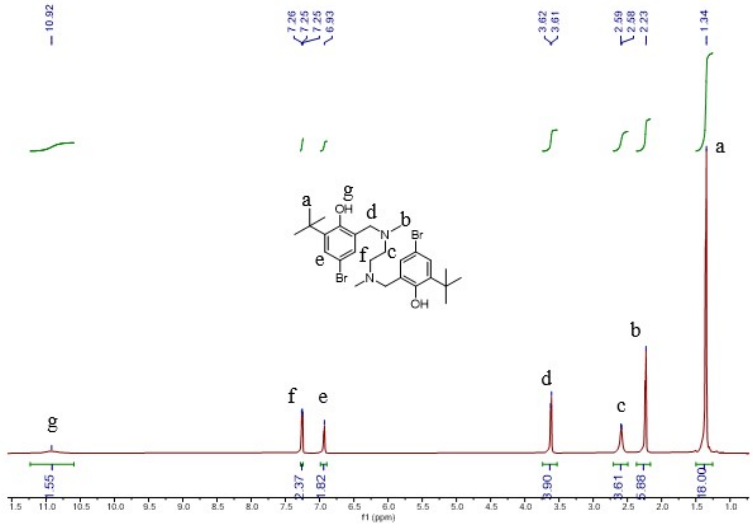

Figure S12. ^{1}H NMR spectrum of **^{Bu}ONNO^{Br}-H** in $CDCl_3$

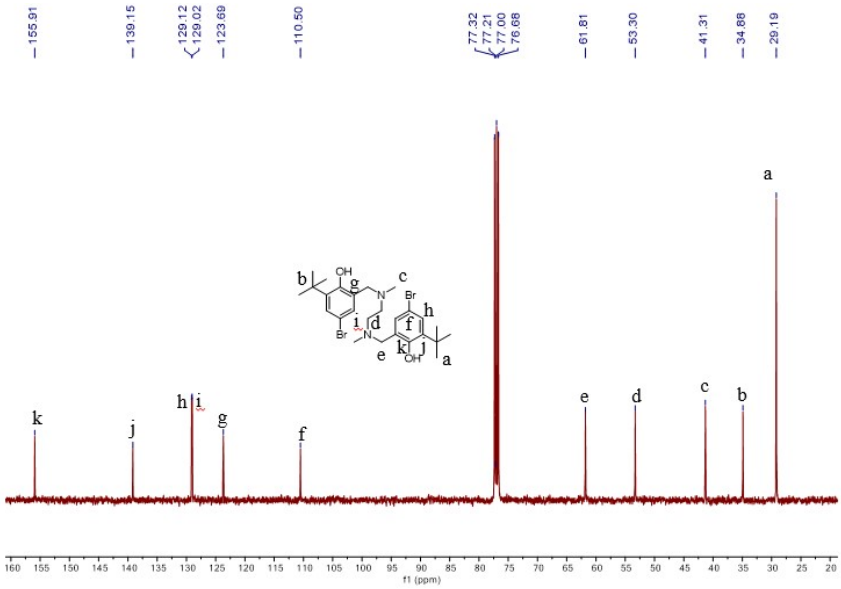

Figure S13. ^{13}C NMR spectrum of **^{Bu}ONNO^{Br}-H** in $CDCl_3$

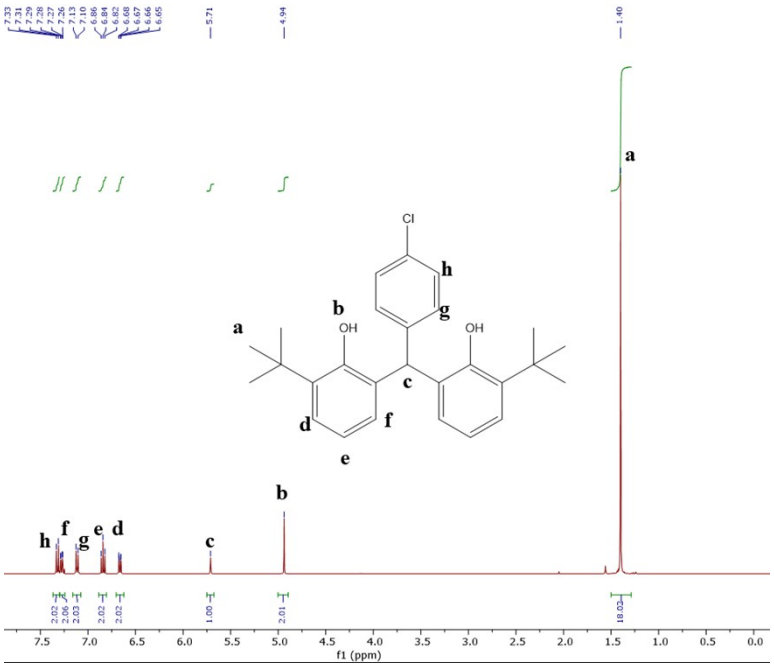

Figure S14. ^{1}H NMR spectrum of **OO^{H}-H** in $CDCl_3$

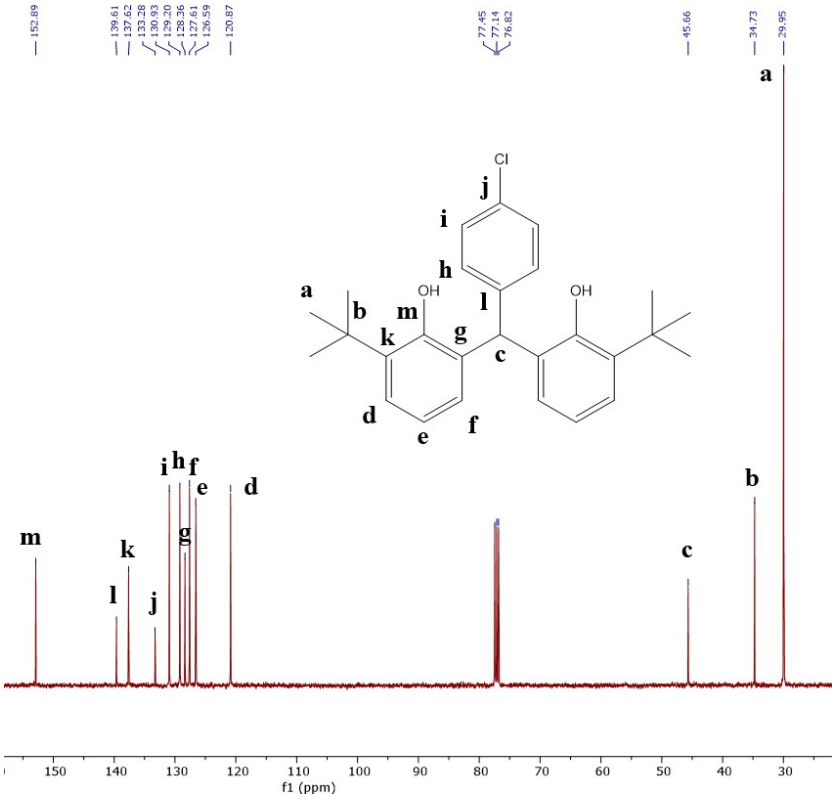

Figure S15. ^{13}C NMR spectrum of **OO^{H}-H** in $CDCl_3$

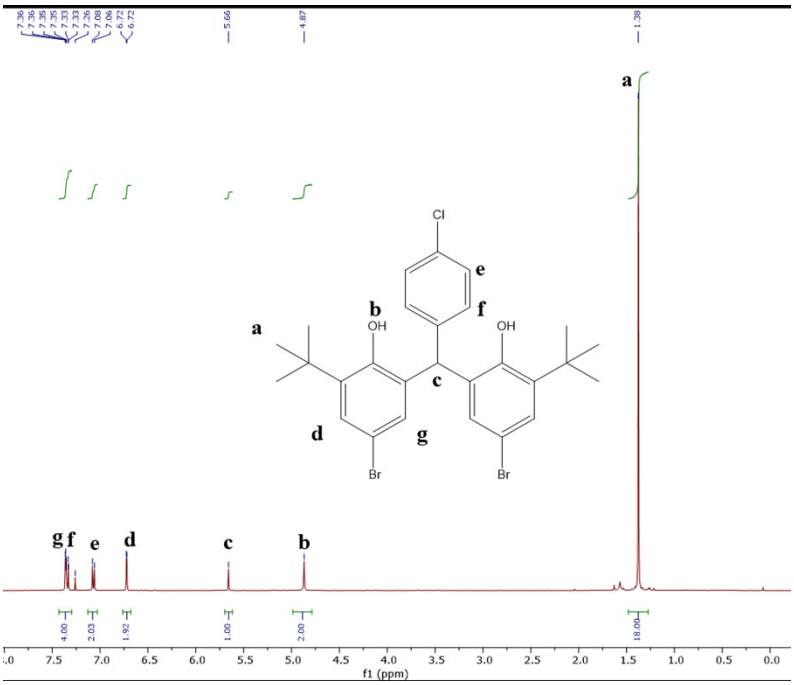

Figure S16. ^{1}H NMR spectrum of **OO^{Br}-H** in $CDCl_3$

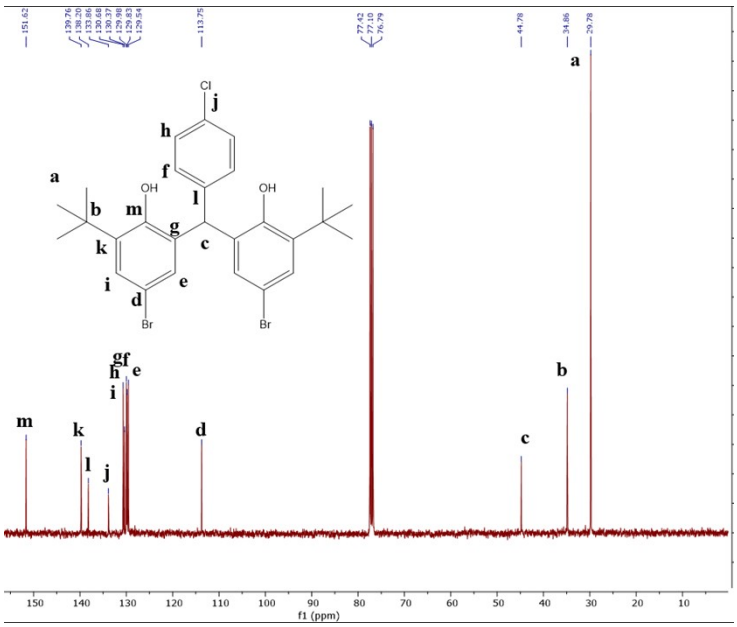

Figure S17. ^{13}C NMR spectrum of **OO^{Br}-H** in $CDCl_3$

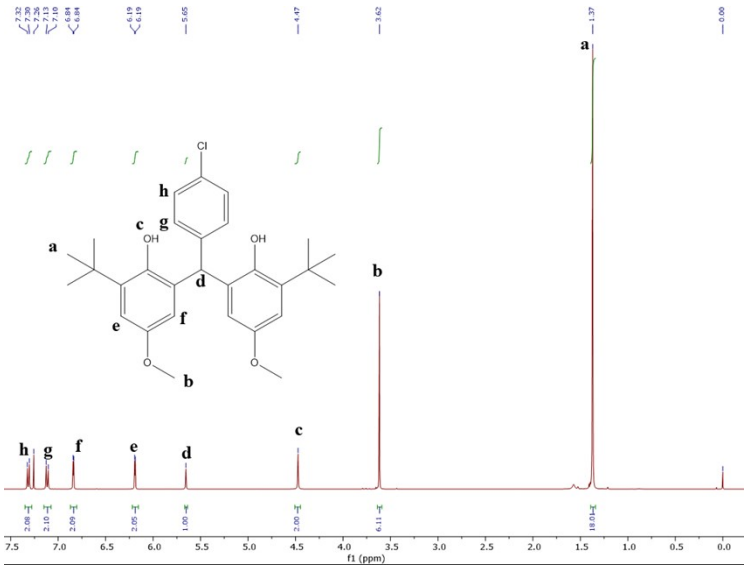

Figure S18. ^{1}H NMR spectrum of **OO^{OMe}-H** in $CDCl_3$

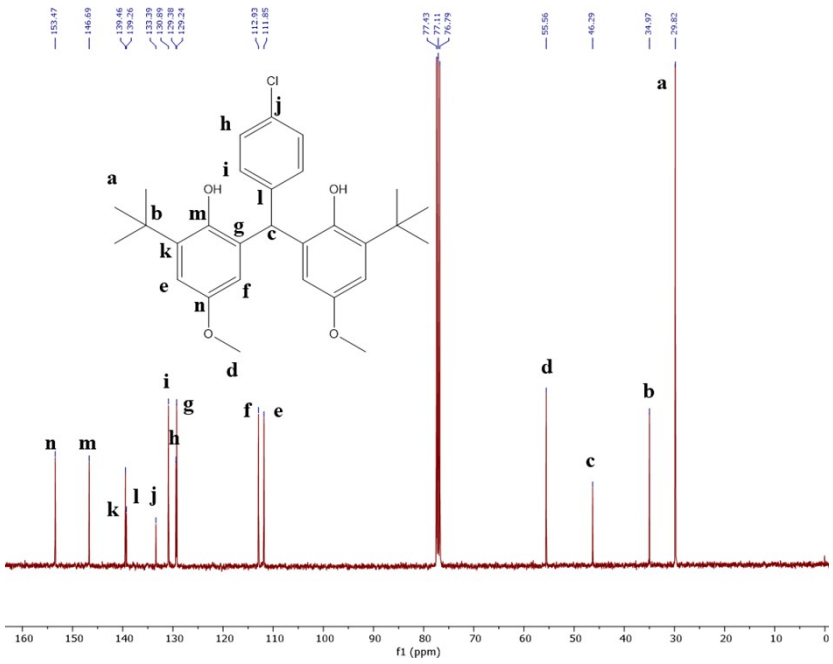

Figure S19. ^{13}C NMR spectrum of **OO^{OMe}-H** in $CDCl_3$

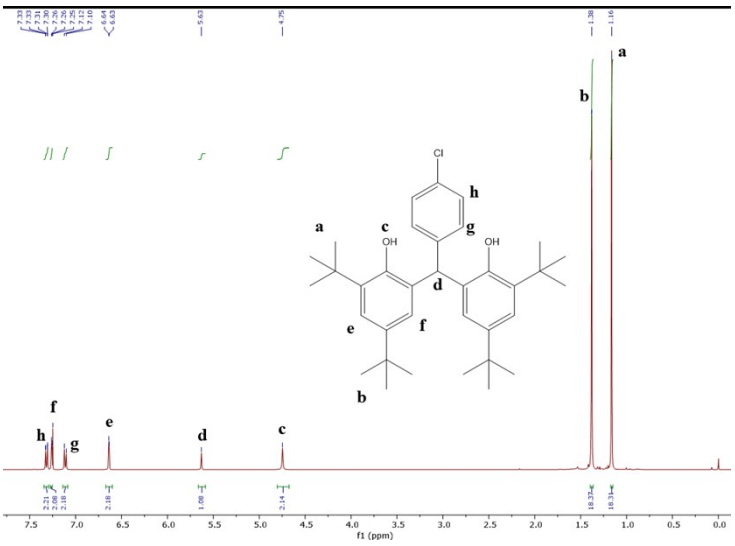

Figure S20. ^{1}H NMR spectrum of **OO^{Bu}-H** in $CDCl_3$

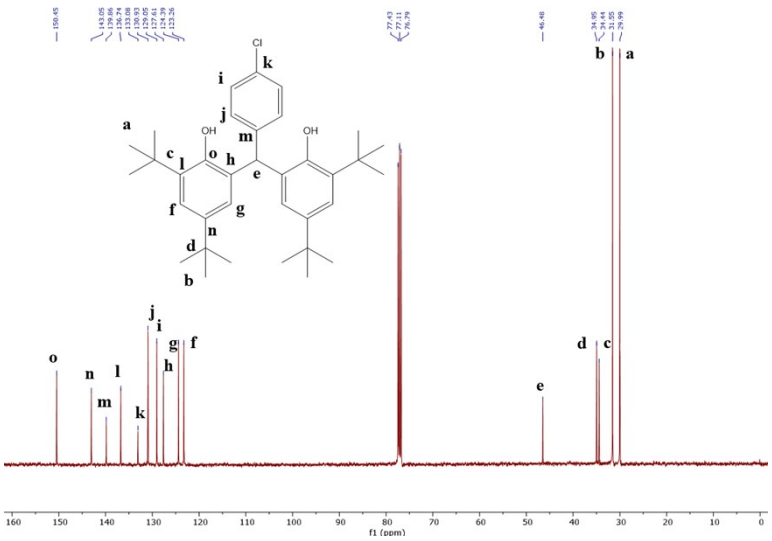

Figure S21. ^{13}C NMR spectrum of **OO^{Bu}-H** in $CDCl_3$

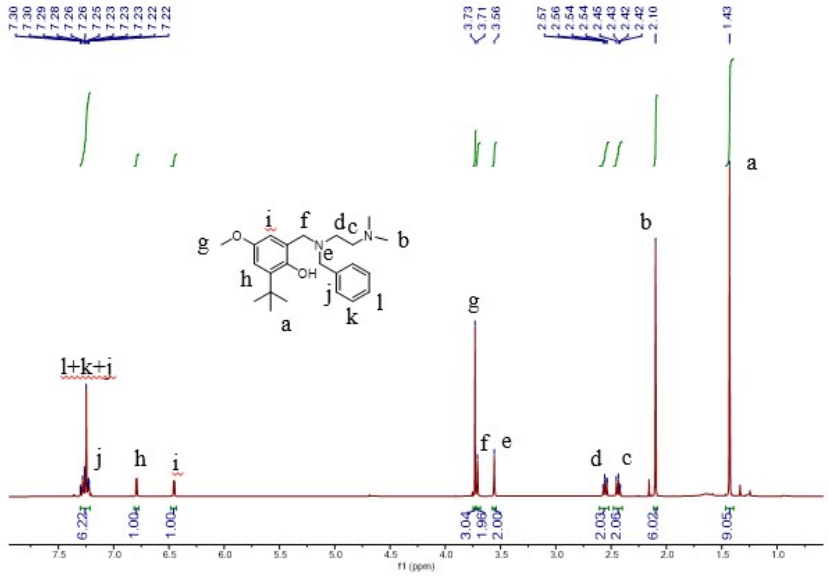

Figure S22. ^{1}H NMR spectrum of **NNO^{OMe}-H** in $CDCl_3$

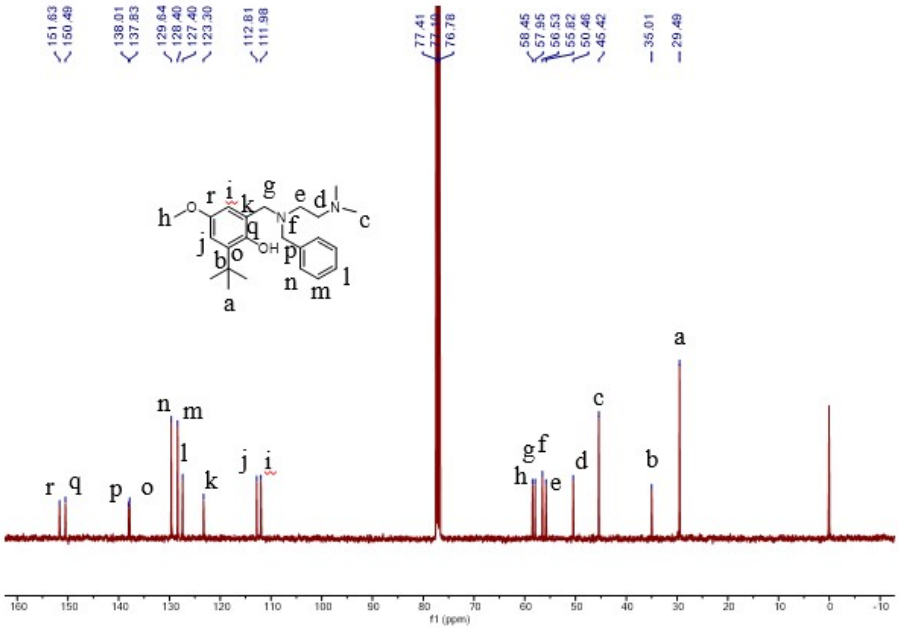

Figure S23. ^{13}C NMR spectrum of **NNO^{OMe}-H** in $CDCl_3$

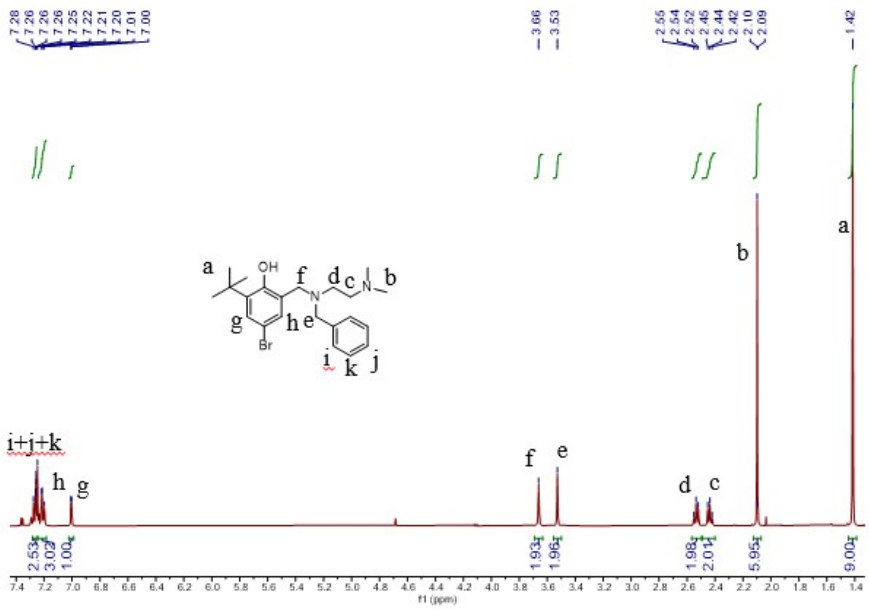

Figure S24. ^{1}H NMR spectrum of **NNO^{Br}-H** in $CDCl_3$

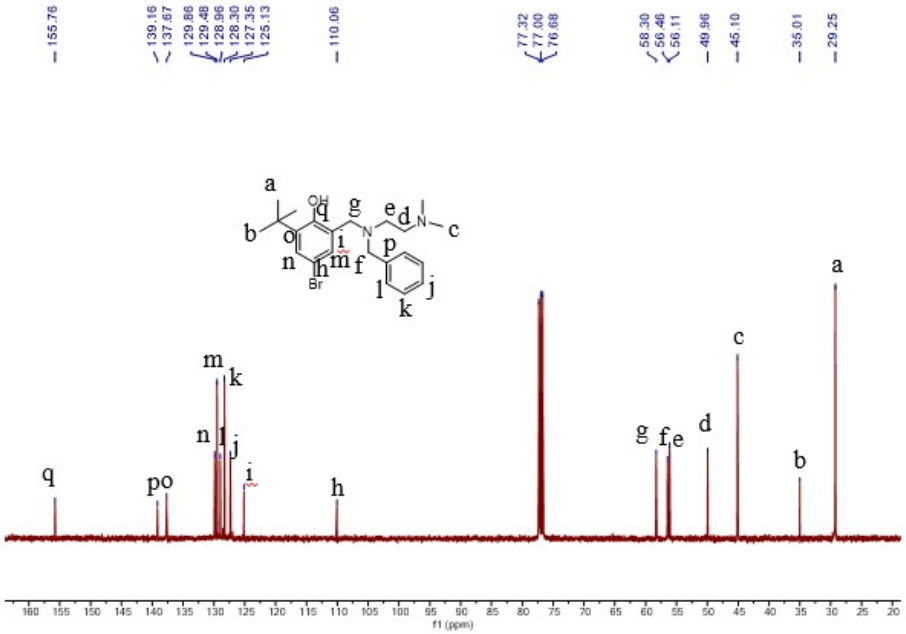

Figure S25. ^{13}C NMR spectrum of **NNO^{Br}-H** in $CDCl_3$

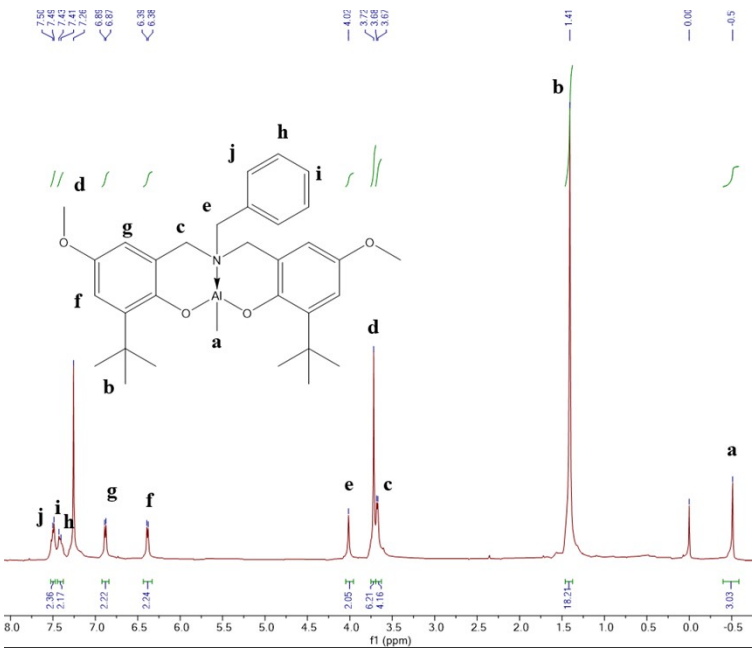

Figure S26. ^{1}H NMR spectrum of **ONO^{OMe}-Al** in $CDCl_3$

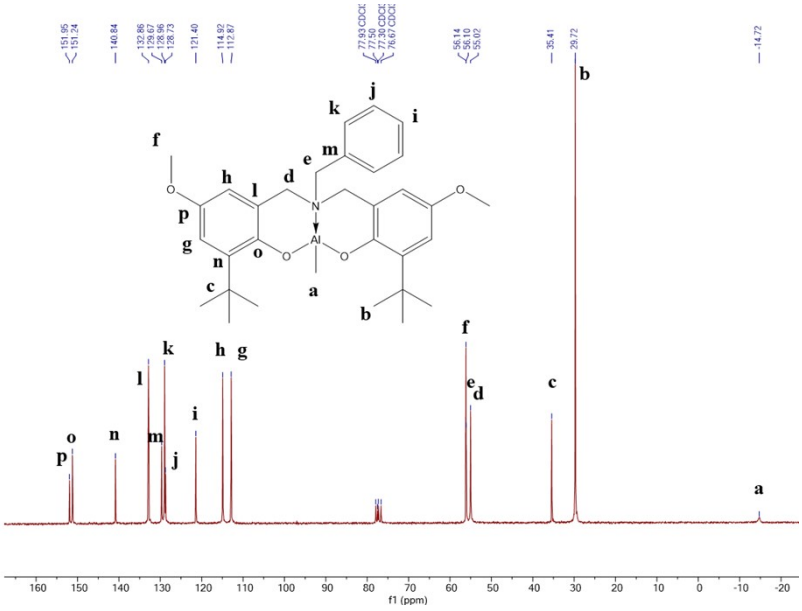

Figure S27. ^{13}C NMR spectrum of **ONO^{OMe}-Al** in $CDCl_3$

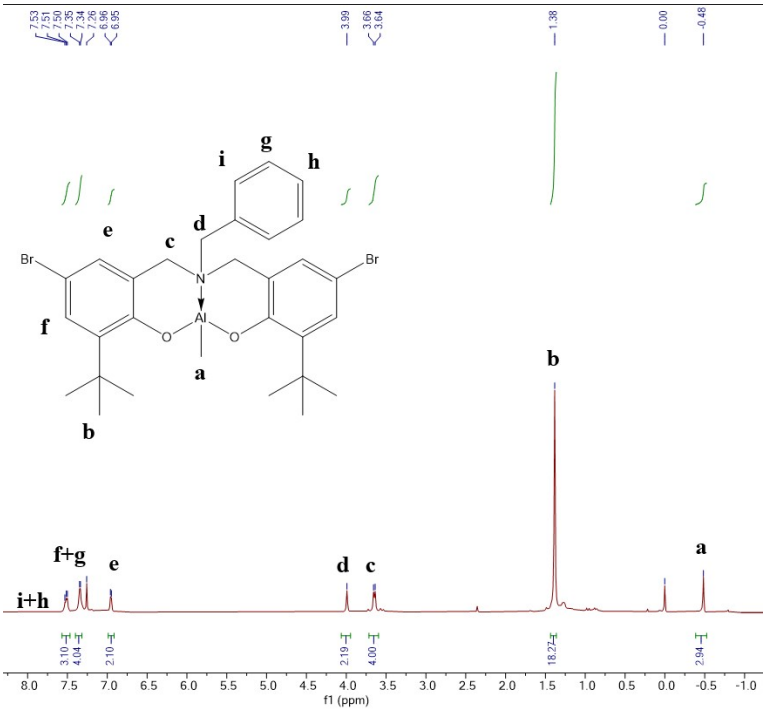

Figure S28. ^{1}H NMR spectrum of **ONO^{Br}-Al** in $CDCl_3$

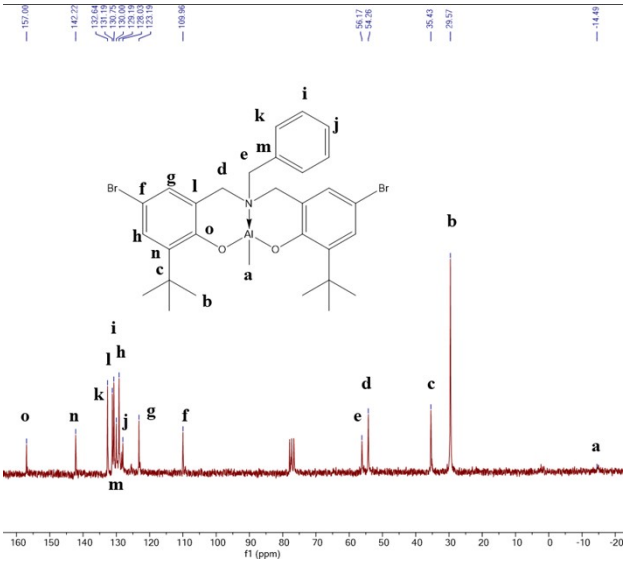

Figure S29. ^{13}C NMR spectrum of **ONO^{Br}-Al** in $CDCl_3$

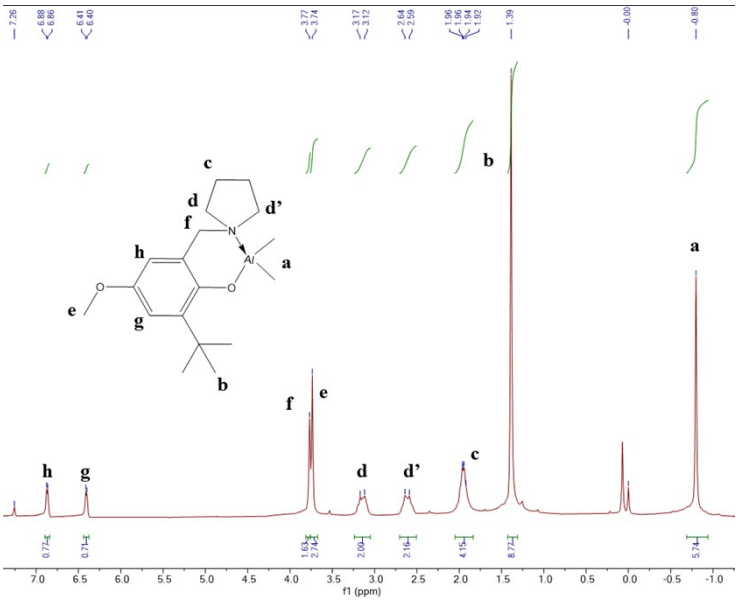

Figure S30. ^{1}H NMR spectrum of **ON^{OMe}-Al** in $CDCl_3$

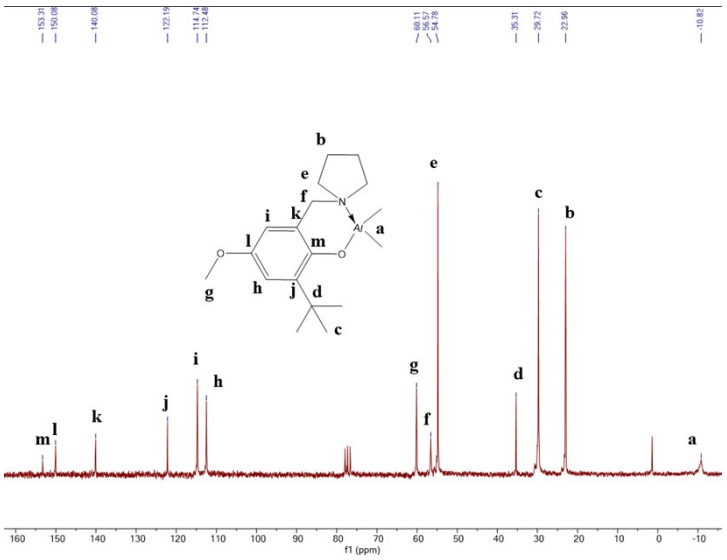

Figure S31. ^{13}C NMR spectrum of **ON^{OMe}-Al** in $CDCl_3$

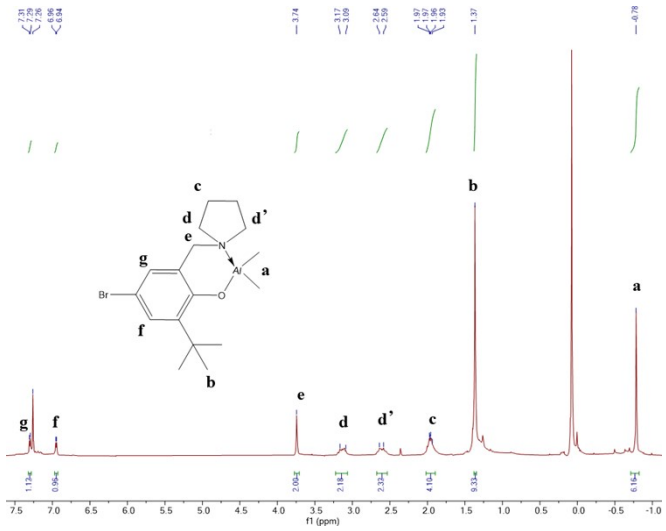

Figure S32. ^{1}H NMR spectrum of **ON^{Br}-Al** in $CDCl_3$

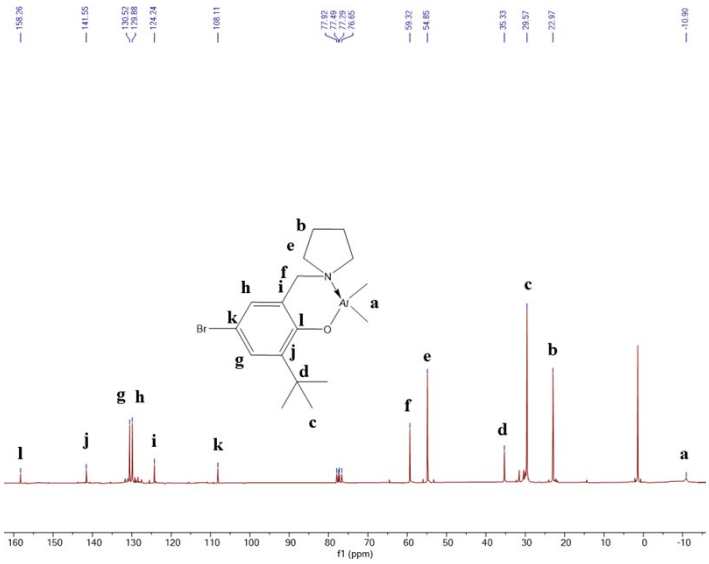

Figure S33. ^{13}C NMR spectrum of **ON^{Br}-Al** in $CDCl_3$

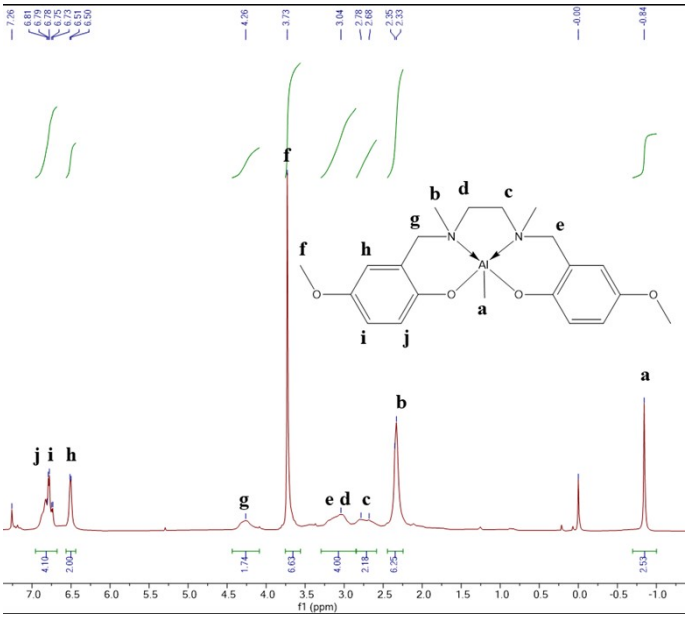

Figure S34. ^{1}H NMR spectrum of **ONNO^{OMe}-Al** in $CDCl_3$

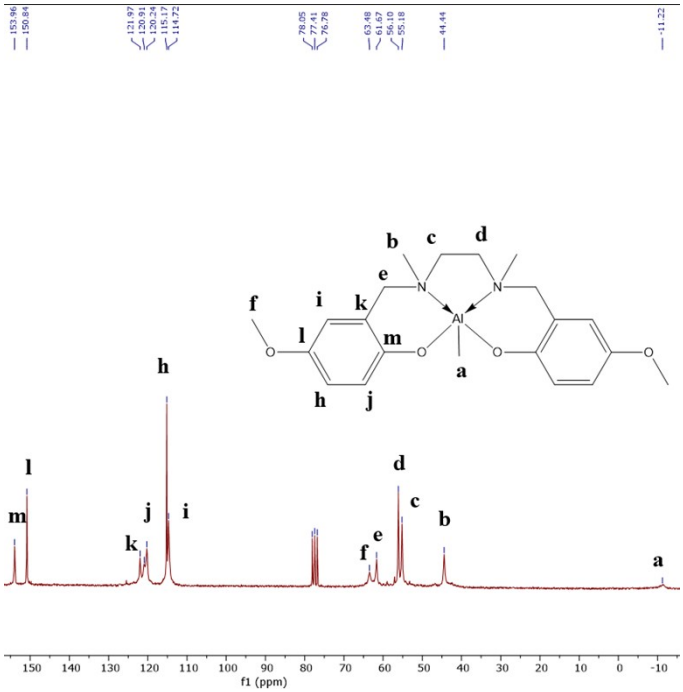

Figure S35. ^{13}C NMR spectrum of **ONNO^{OMe}-Al** in $CDCl_3$

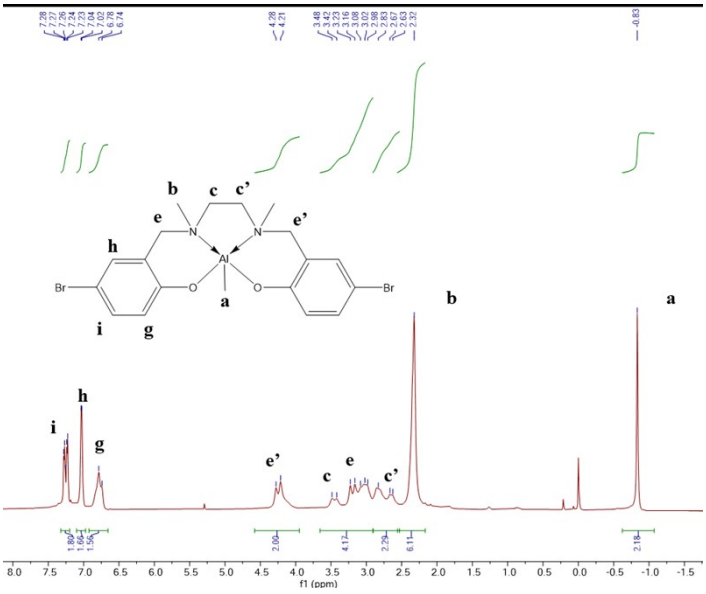

Figure S36. ^{1}H NMR spectrum of **ONNO^{Br}-Al** in $CDCl_3$

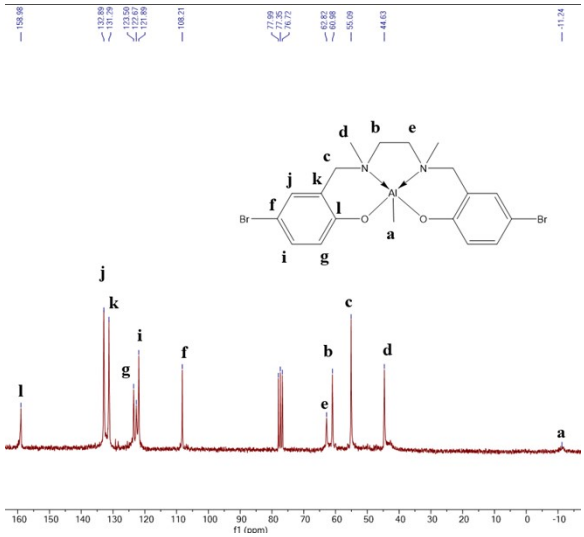

Figure S37. ^{13}C NMR spectrum of **ONNO^{Br}-Al** in $CDCl_3$

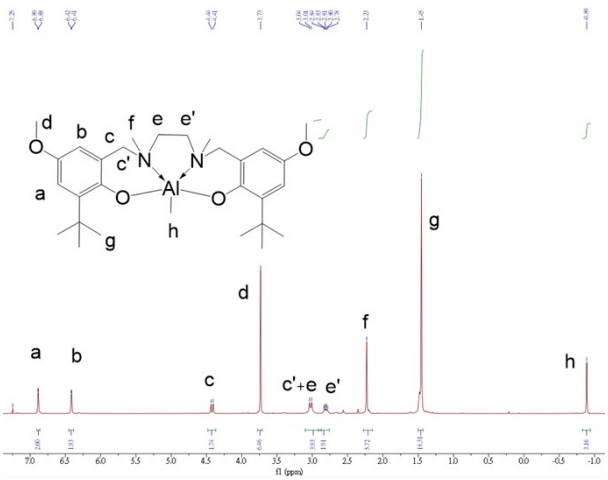

Figure S38. ^{1}H NMR spectrum of **^{Bu}ONNO^{OMe}-Al** in $CDCl_3$

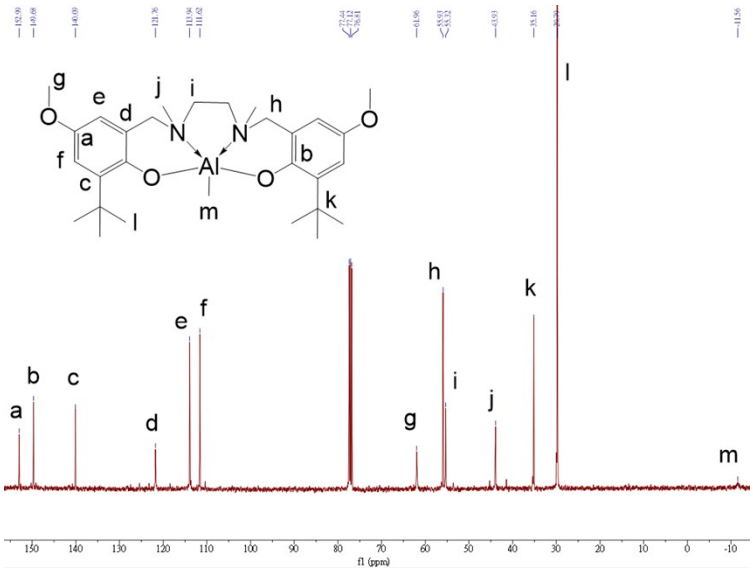

Figure S39. ^{13}C NMR spectrum of **^{Bu}ONNO^{OMe}-Al** in $CDCl_3$

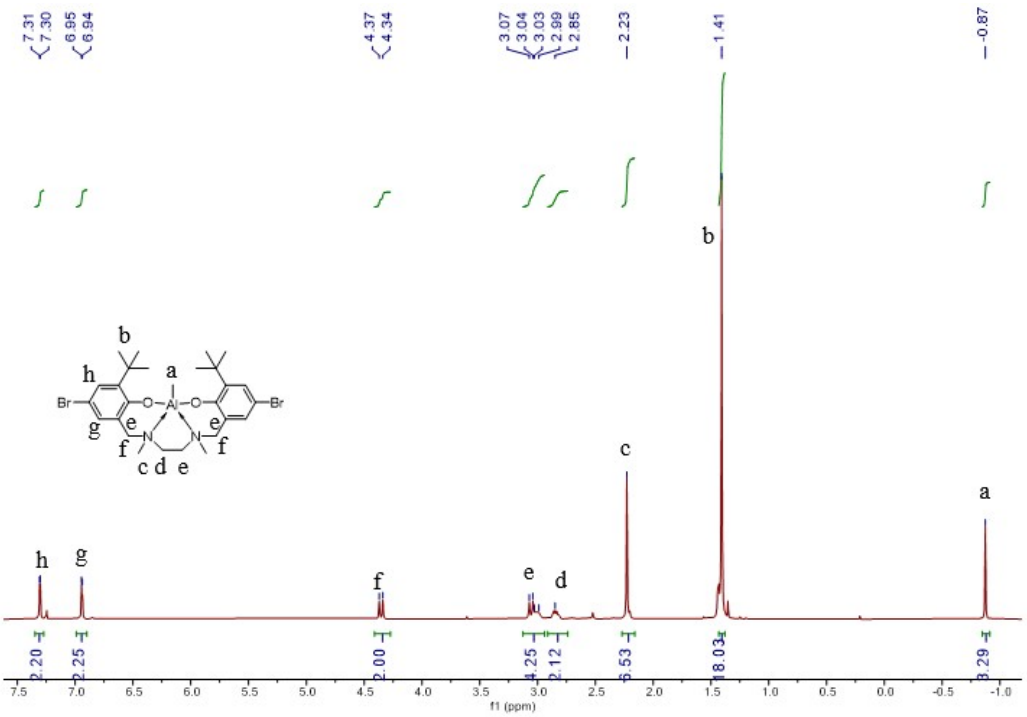

Figure S40. ^{1}H NMR spectrum of **^{Bu}ONNO^{Br}-Al** in $CDCl_3$

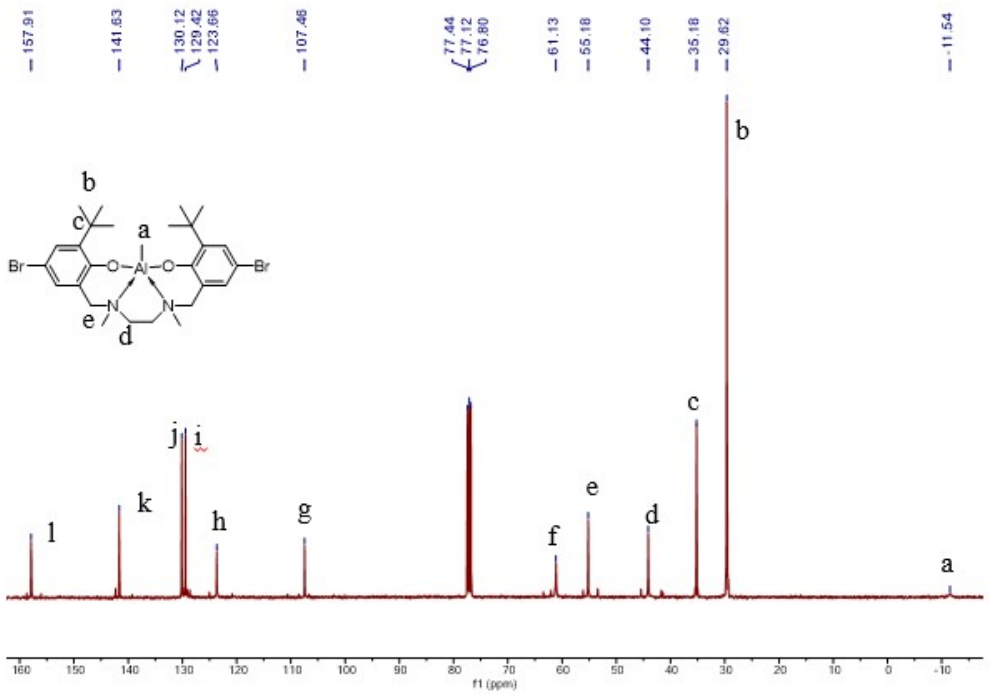

Figure S41. ^{13}C NMR spectrum of **^{Bu}ONNO^{Br}-Al** in $CDCl_3$

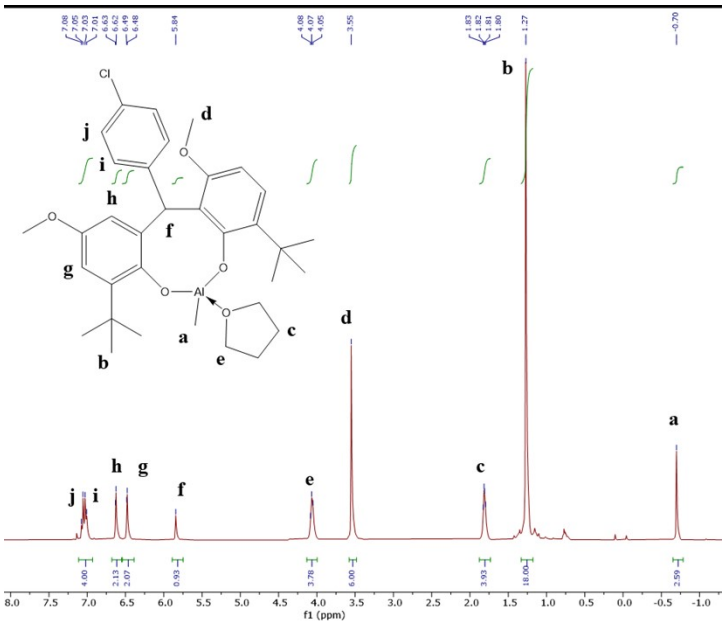

Figure S42. ^{1}H NMR spectrum of **OO^{OMe}-Al** in $CDCl_3$

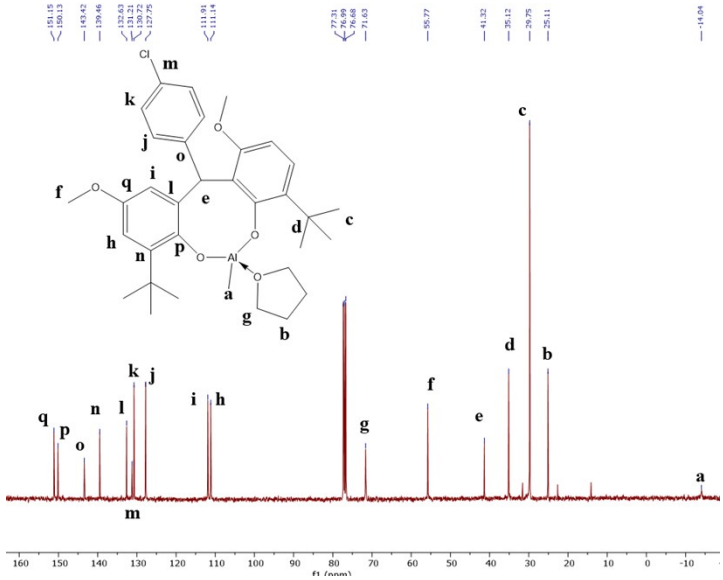

Figure S43. ^{13}C NMR spectrum of **OO^{OMe}-Al** in $CDCl_3$

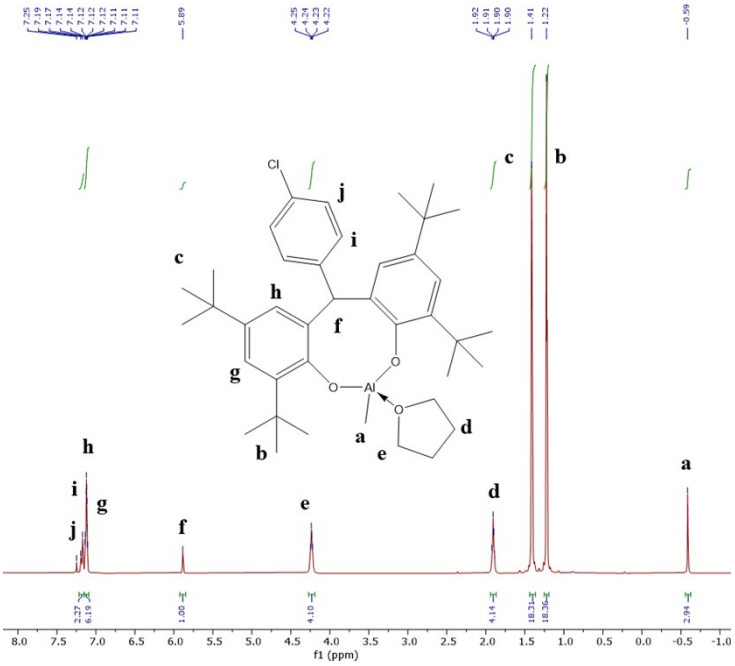

Figure S44. ^{1}H NMR spectrum of **OO^{Bu}-Al** in $CDCl_3$

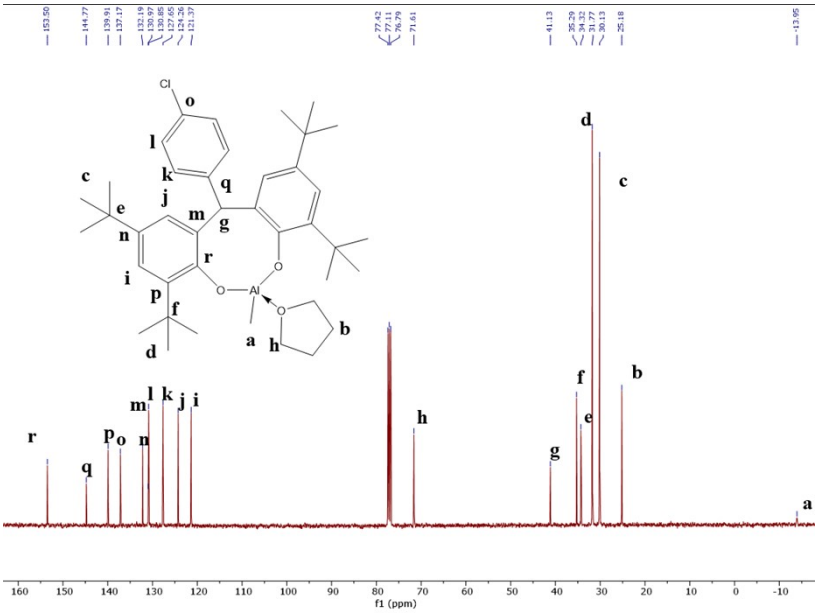

Figure S45. ^{13}C NMR spectrum of **OO^{Bu}-Al** in $CDCl_3$

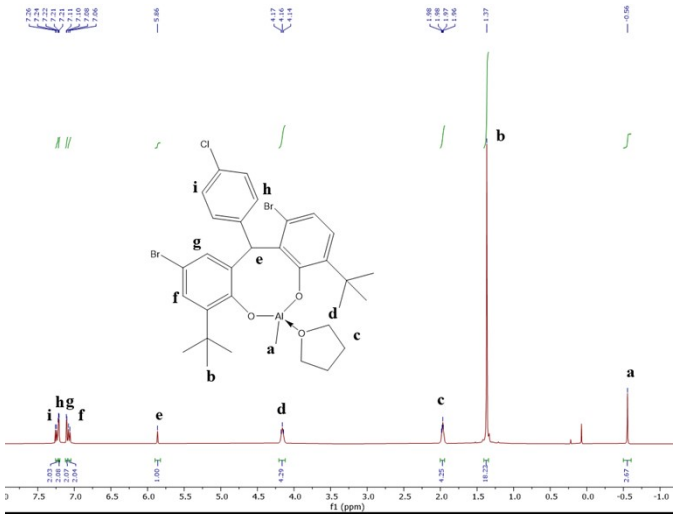

Figure S46. ^{1}H NMR spectrum of **OO^{Br}-Al** in $CDCl_3$

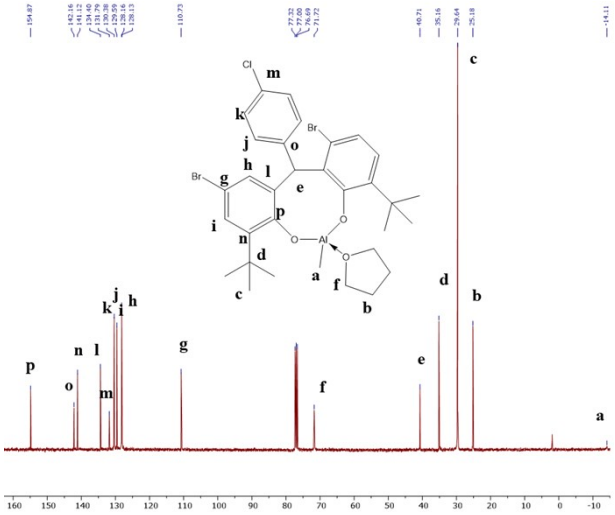

Figure S47. ^{13}C NMR spectrum of **OO^{Br}-Al** in $CDCl_3$

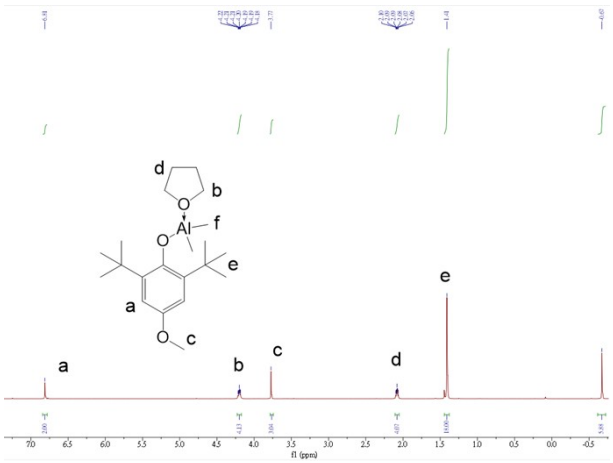

Figure S48. ^{1}H NMR spectrum of **O^{OMe}-Al** in $CDCl_3$

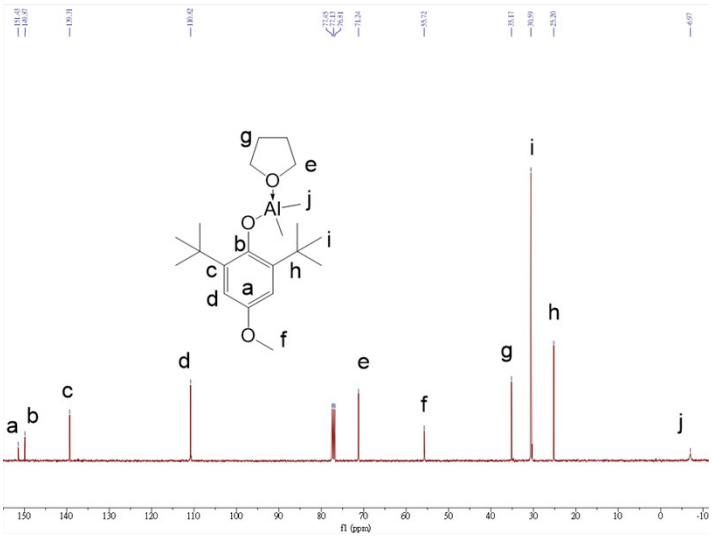

Figure S49. ^{13}C NMR spectrum of **O^{OMe}-Al** in $CDCl_3$

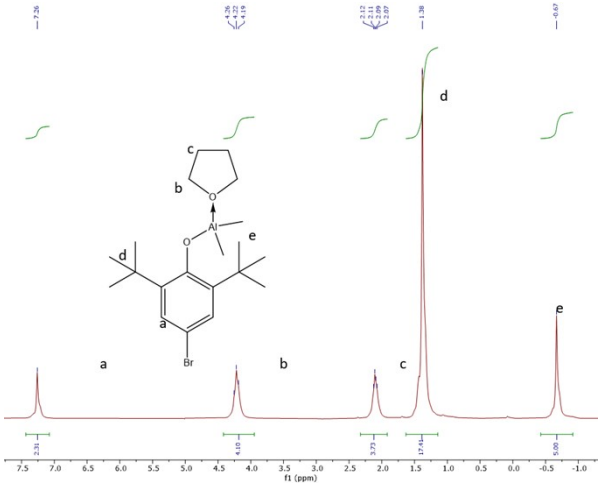

Figure S50. ^{1}H NMR spectrum of **O^{Br}-Al** in $CDCl_3$

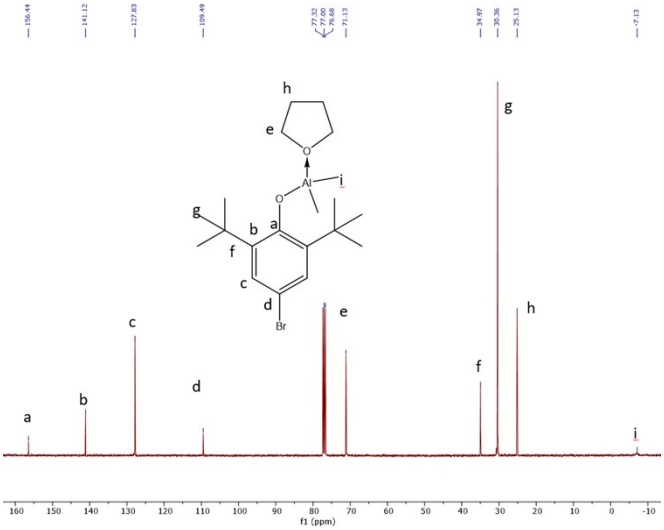

Figure S51. ^{13}C NMR spectrum of **O^{Br}-Al** in $CDCl_3$

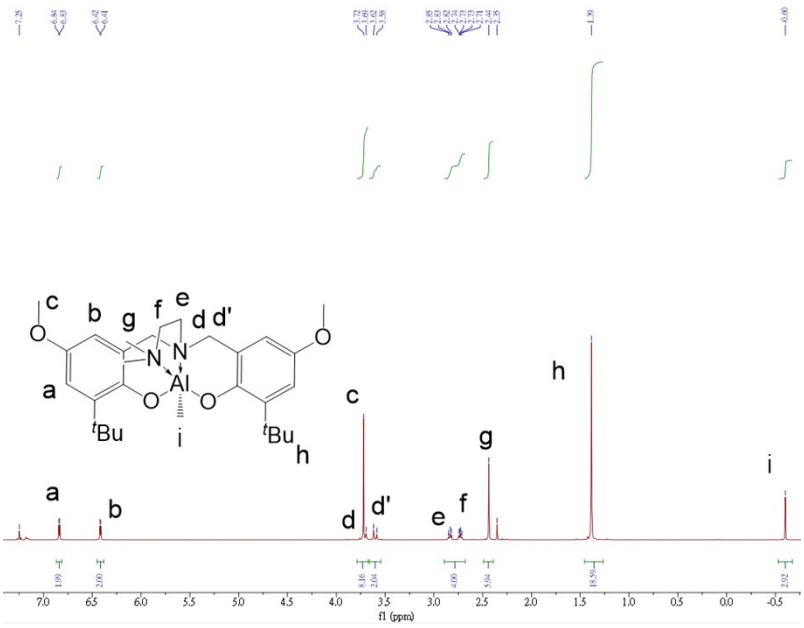

Figure S52. ^{1}H NMR spectrum of **NNOO^{OMe}-Al** in $CDCl_3$

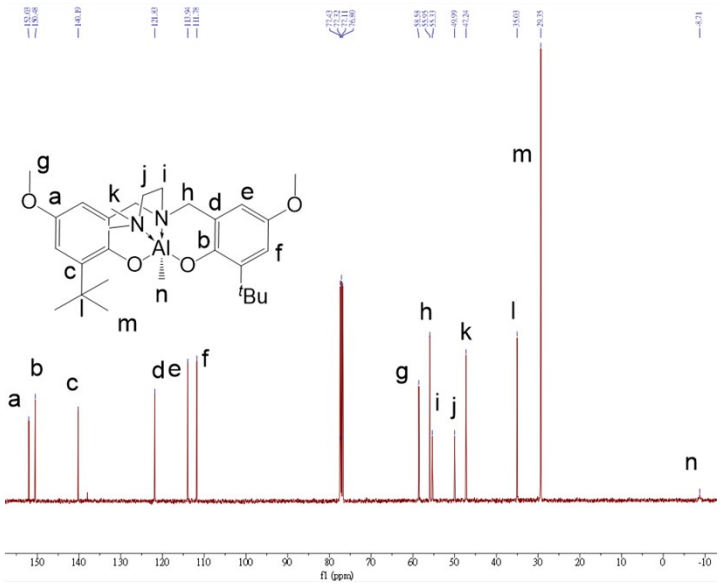

Figure S53. ^{13}C NMR spectrum of **NNOO^{OMe}-Al** in $CDCl_3$

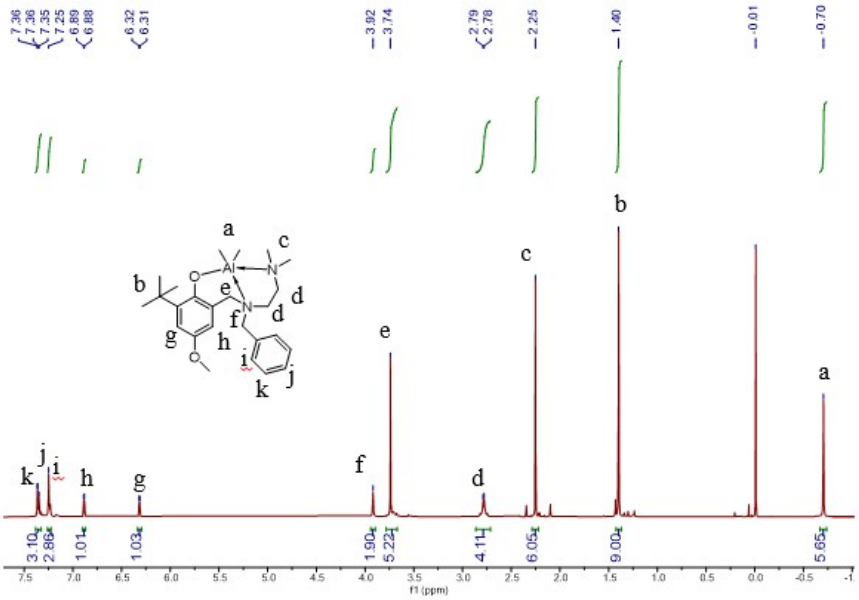

Figure S54. ^{1}H NMR spectrum of **NNO^{OMe}-Al** in $CDCl_3$

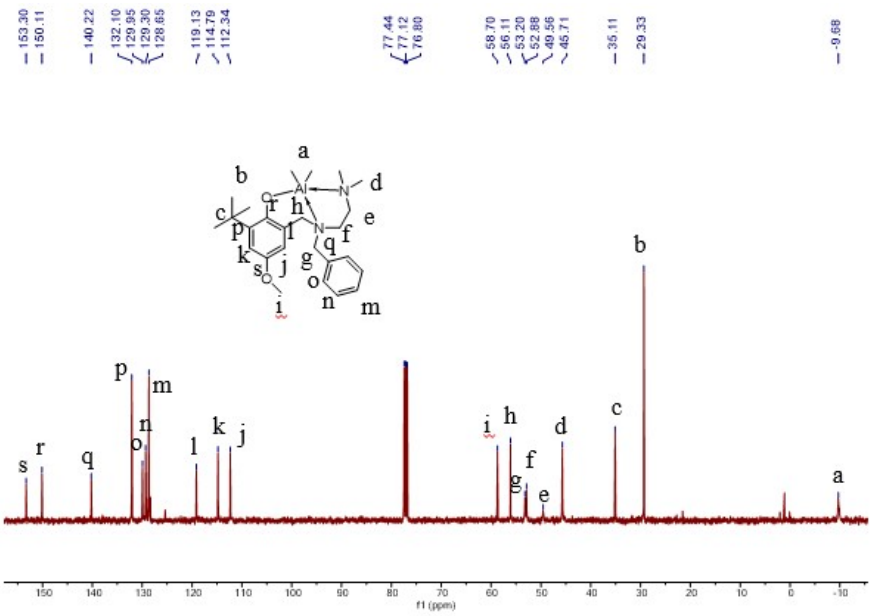

Figure S55. ^{13}C NMR spectrum of **NNO^{OMe}-Al** in $CDCl_3$

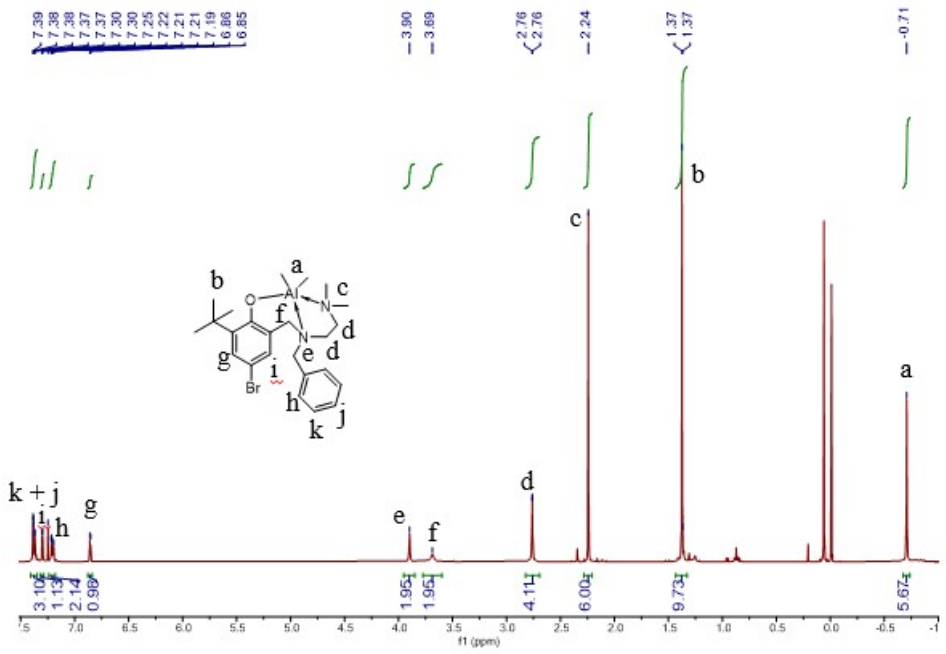

Figure S56. ^{1}H NMR spectrum of **NNO^{Br}-Al** in $CDCl_3$

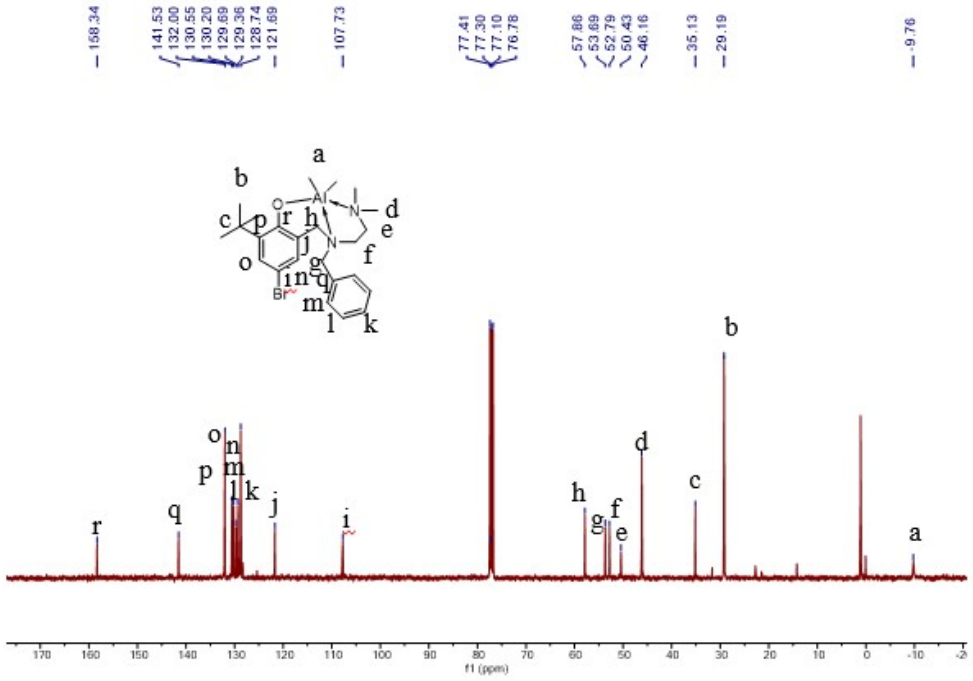

Figure S57. ^{13}C NMR spectrum of **NNO^{Br}-Al** in $CDCl_3$

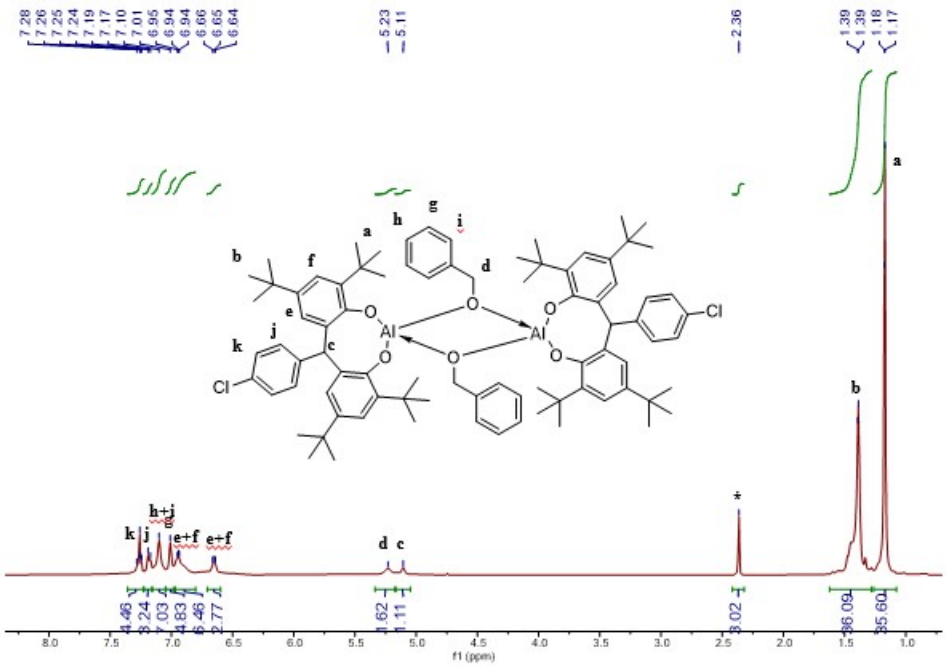

Figure S58. ^{1}H NMR spectrum of **(OO^{Bu}-AlOBn)$_2$** in $CDCl_3$

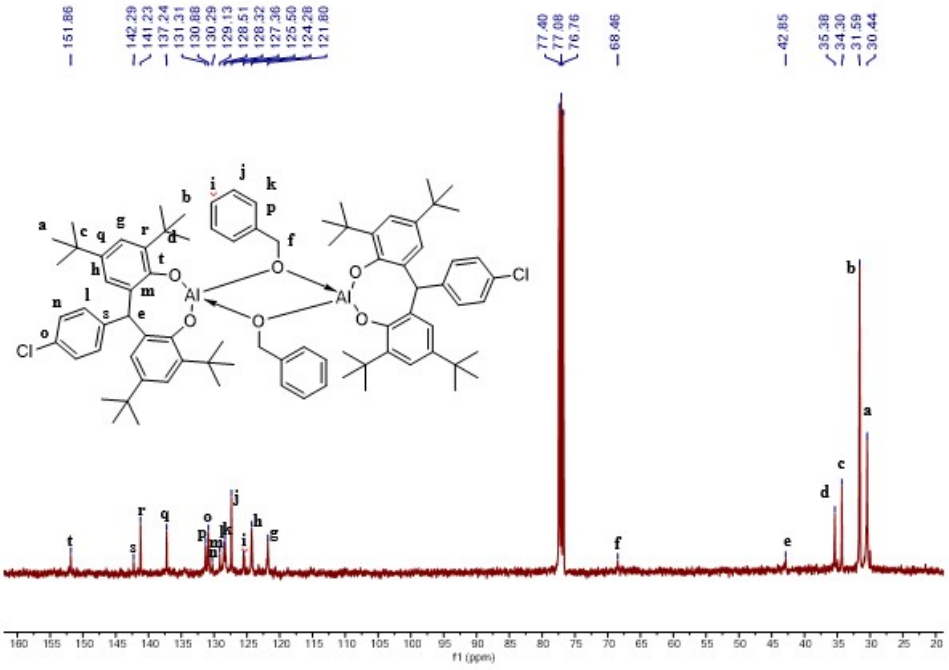

Figure S59. ^{13}C NMR spectrum of **(OO^{Bu}-AlOBn)$_2$** in $CDCl_3$

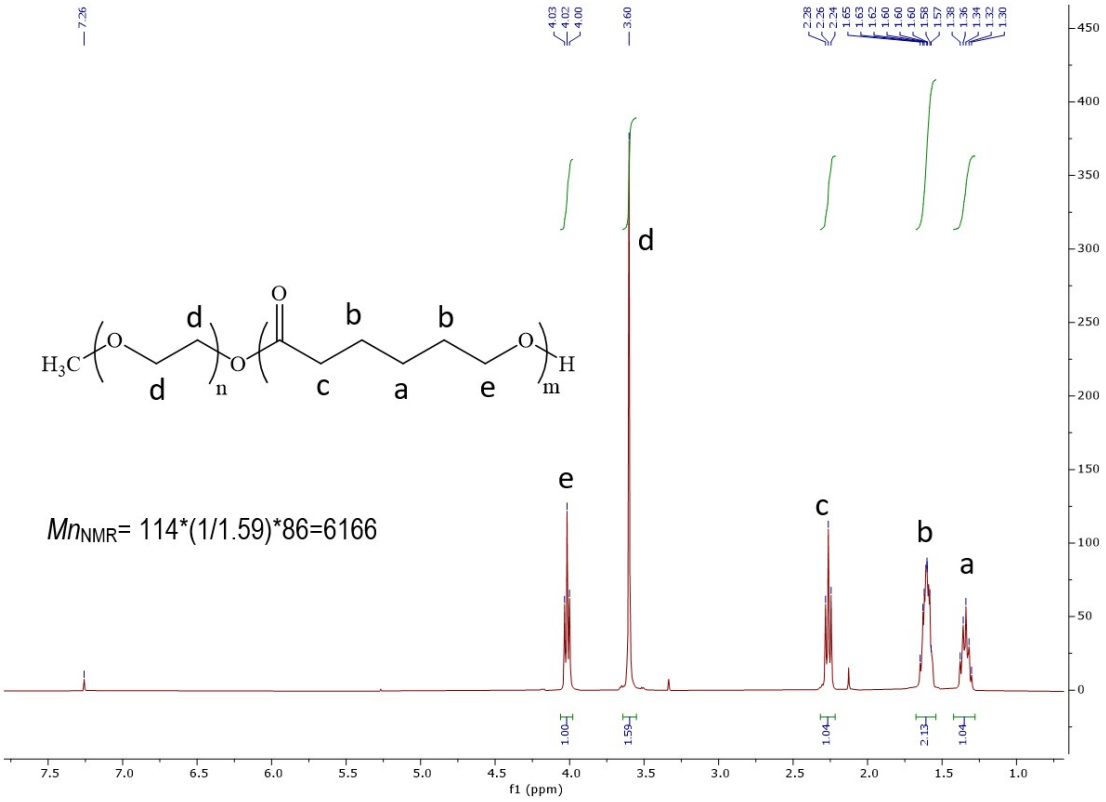

Figure S60. ^{1}H NMR spectrum of *m*PEG-b-PCL copolymer (entry 6 of **Table 2**) in $CDCl_3$

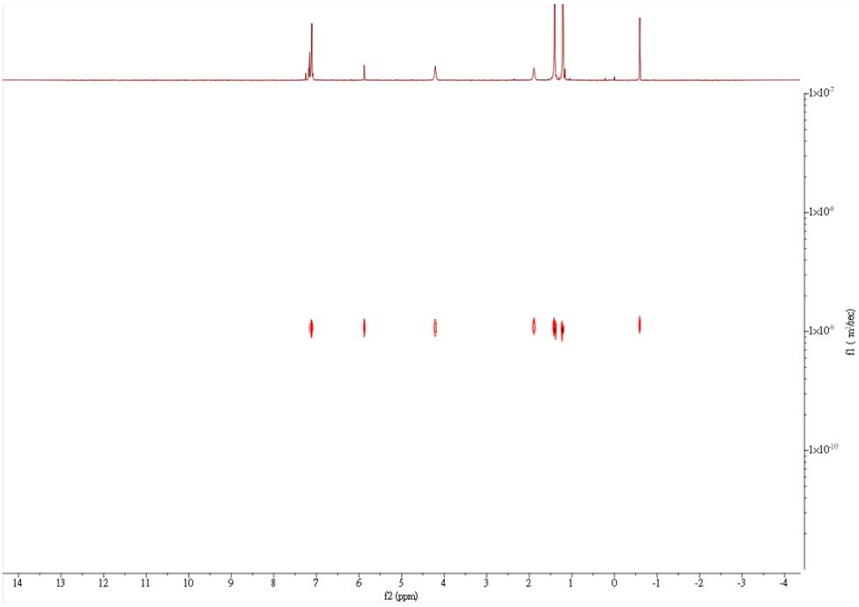

Figure S61. ^{1}H DOSY NMR spectrum of **OO^{Bu}-Al** (D = 11x10^{-10} m^2/s)

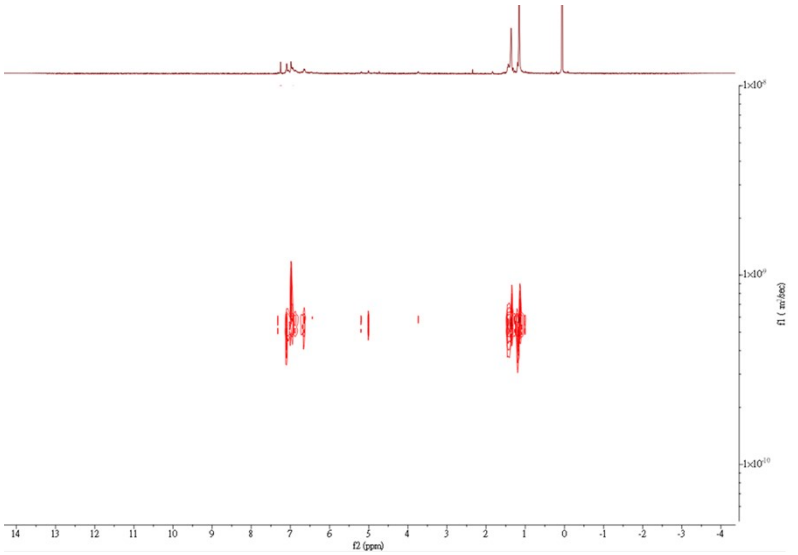

Figure S62. ^{1}H DOSY NMR spectrum of **(OO^{Bu}-AlOBn)$_2$** (D = 6.01 x10^{-10} m^2/s)

Density functional theory calculation of the CL polymerization mechanism by using OO^{OMe}-Al as a Catalyst

The density functional theory (DFT) calculations for the theoretical study are carried out by the Gaussian 09E program package.[1] For dimer-tetramer interconversions, the ligand structures in the calculation are simplified to reduce the calculation loading using methyl groups to substitute *t*-Bu groups on the phenols of the chelating ligand, hydrogen atom to substitute the central 4-chlorophenyl group and methoxide ligands to replace benzyloxide ligands. For polymerization reaction mechanisms, the OO^{OMe} ligand is employed as the chelating ligand, and methoxide ligands are selected as the monodentate alkoxide ligands and the reaction initiator. All the calculations are carried under B3LYP level with 6-31G(d) basis sets.

Table S5. The abbreviations of specific atoms mentioned in the DFT study

Dimer-B

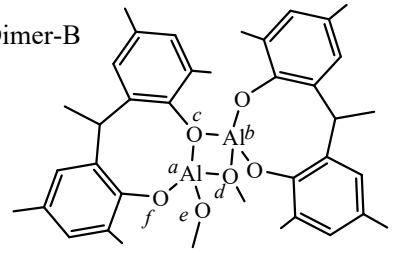

CL

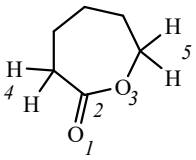

label	Specific atoms in the structures	Abbreviation
a		Al-1
b		Al-2
c	Bridging phenoxide oxygen	$O^{\mu\text{-Ph}}$
d	Bridging methoxide oxygen	$O^{\mu\text{-Me}}$
e	Terminal methoxide oxygen	$O^{tm\text{-Me}}$
f	Non-bridging phenoxide oxygen	$O^{nb\text{-Ph}}$
1	The carbonyl oxygen of CL	O^{car}
2	Carbonyl carbon of CL	C^{car}
3	Ester oxygen of CL	O^{est}
4	α-hydrogen of CL	H^{α}
5	ω-hydrogen of CL	H^{ω}

From literatures,[2-5] the catalyst is known to have a stable di-μ_2-alkoxide bridged dimeric structure (**Dimer-A)** in solid states (**Figure 5**). In solution, it is expected to form phenoxide bridged isomers, including **Dimer-B** and **Dimer-C**. **Dimer-B** has an μ_2-alkoxide-μ_2-phenoxide unsymmetrical structure in which one less crowded Al atom possesses a terminal alkoxide ligand with relatively larger open space to accept a substrate, and three bulky ortho-substituted phenoxide ligands surround the other Al. **Dimer-C** has di-μ_2-phenoxide bridged structure with one terminal alkoxide ligand on each Al but almost no space around the metal centers for extra ligand coordination. Due to the higher electron donating ability and the lower steric effect of the alkoxide ligands compared to that of the ortho-substituted phenoxide ligands, **Dimer-A** should be more stable than **Dimer-B,** which should be more stable than **Dimer-C**. Moreover, the anti-form of the dimers should be more stable than the syn-form due to the repulsion between the bulky groups. However, in Dimer-B, the anti-structure has higher energy than the syn structure because the twisted unsymmetric structure forces a *t*-Bu group of one complex to approach the other. The free energy of the three isomers are anti-**Dimer-A** (set as 0.00 kcal mol^{-1}) < syn-**Dimer-A** (2.68 kcal mol^{-1}) < anti-**Dimer-B** (16.44 kcal mol^{-1}) < syn-**Dimer-C** (24.04 kcal mol^{-1}) < anti-**Dimer-C** (27.54 kcal mol^{-1}) < anti-**Dimer-B** (28.10 kcal mol^{-1}).

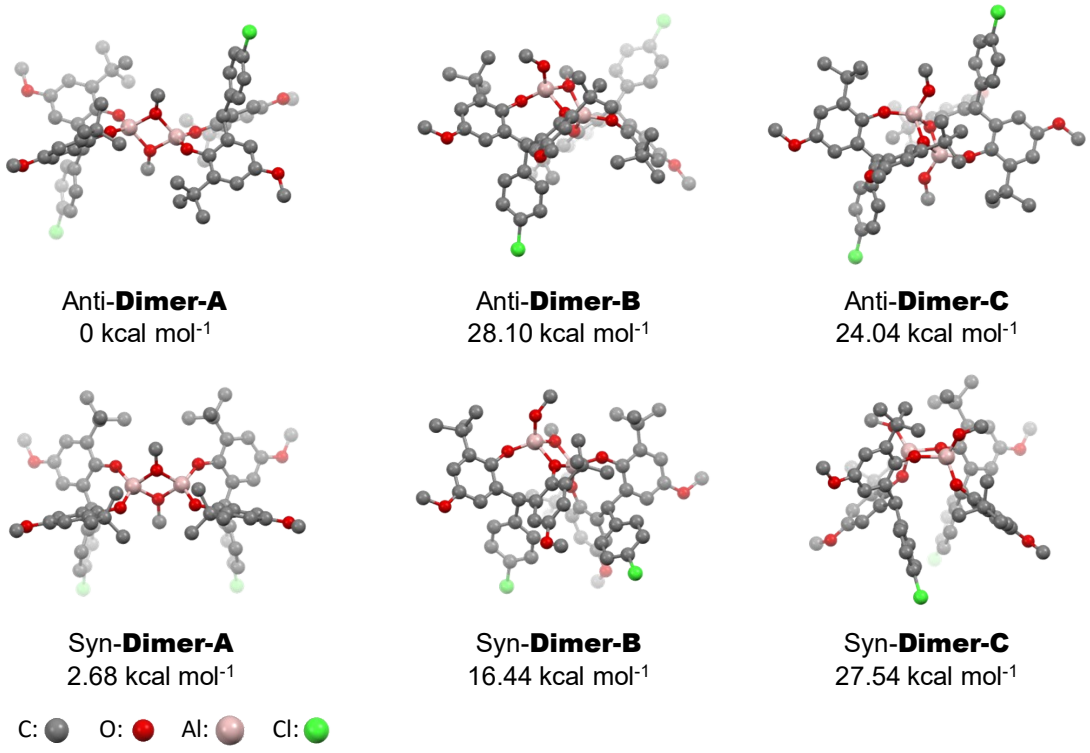

Figure S63. The possible dimeric structures of the catalyst

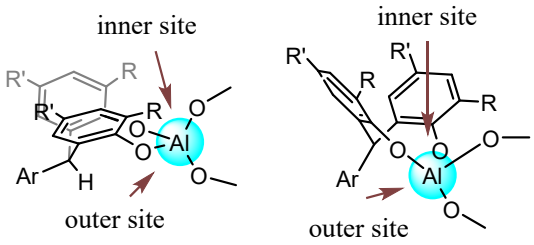

Figure S64. The illustration of the inner and outer sites on Al center. (side view: left; front view: right)

Two CL coordination sites can be found on each Al atom of these three isomers, as shown in **Figure 51**. One is the coordination site at the chelating ligand's inner side (inner site). The other is beside the chelating ligand (outer site). Because **Dimer-A** and **Dimer-C** are symmetrical structures, only two coordination sites exist. In **Dimer-B**, there are four coordination sites. The inner coordination sites are more accessible for CL than the outer sites due to the flat aromatic structure of the chelating ligand offering larger open spaces between two phenoxide coordination points. As shown in **Table 6**, the coordination sites on both Al atoms of **Dimer-A** and the Al-1 of **Dimer-B** have lower coordination energies than those of the Al-2 of **Dimer-B** and both Al of **Dimer-C**, indicating that CL can be more readily access to the inner sites of **Dimer-A** and **Dimer-B**'s Al-1. Moreover, from the reorganization energies of structures, the inner site on **Dimer-B**'s Al-1 can accept CL with smaller structural changes than does on **Dimer-A**. Furthermore, because there is no terminal alkoxide ligand on **Dimer-A**, bond breaking of Al-$O^{\mu\text{-Me}}$ should proceed before the addition reaction between alkoxide anion and CL. The energy required for this process is around 23 kcal mol^{-1}, larger than the energy difference between **Dimer-A** and **Dimer-B**. Based on the information above, the inner site of the **Dimer-B**'s Al-1 atom has the highest chance of being the catalytic site for the ring-opening reaction.

Therefore, to initiate the reaction, the catalyst must convert to **Dimer-B** in the first step of the catalytic reaction. This conversion can possibly be achieved through a tetranuclear species **T**, as shown in **Scheme 1**. **T** is formed by a ring expansion process in which an Al-O^{Ph} unit of one **Dimer-A** complex (complex α) is inserted into the O-Al-O-Al 4-membered ring of another **Dimer-A** complex (complex β) to generate a new 6-membered O^{Me}-Al-O^{Ph}-Al-O^{Me}-Al ring. After that, one single-Al-bounded $O^{nb\text{-}Ph}$ on complex α migrates to and shares with its neighboring Al on complex α to form a bridge phenoxide. Meanwhile, complex β is dissociated from complex α to finish the transformation process to convert complex α from **Dimer-A** to **Dimer-B**. Although this interconversion involving too many atoms and the direct calculation applied to these structures is challenging, simplified simulations are still

conducted to offer hints to help us understand this process. When para substitutional groups are changed from Br to H, the energy gaps between **T** and **Dimer-A** reduce 2.52 kcal mol^{-1}. When OMe is used to replace H, the energy gaps further reduce 2.00 kcal mol^{-1}. This indicates that the electron-donating substitutional group on the phenol groups of the chelating ligand can reduce the transformation energy barrier from **Dimer-A** to **Dimer-B**. This is one key reason to explain the difference in activity between OO^{OMe} and OO^{Br} in the catalytic reactions.

Table S6. The coordination energy of CL on catalysts[a]

	Dimer-A		**Dimer-B**			**Dimer-C**	
Coordination site	inner	outer	inner-1	outer-1	inner-2	inner	outer
CE[b]	-10.07	-5.16	-10.14	-7.10	6.73	-4.05	2.81
RE[c]	17.11	21.77	15.87	17.35	30.59	14.56	23.72
O(CL)-Al (Å)	2.005	2.026	1.990	2.053	2.019	2.072	2.026
CLBE[d]	-27.18	-26.93	-26.01	-24.45	-23.86	-18.61	-20.91

a. The energies in this table are the electronic energies of the structures in kcal mol^{-1}. The catalysts used to evaluate the energies are the more stable forms (anti-**Dimer-A**, syn-**Dimer-B**, and anti-**Dimer-C**)

b. Coordination energy (CE) = $E^{complex\text{-}CL} - E^{complex}$

c. Reorganization energy (RE) = $E^{complex\text{-}CL(CL\text{-}omitted)} - E^{complex}$ ($E^{complex\text{-}CL(CL\text{-}omitted)}$ is evaluated from the single point energy calculation by omitting CL from the optimized complex-CL.

d. CL binding energy (CLBE) = Coordination energy - Reorganization energy

Scheme S1. The interconversion from **Dimer-A** to **Dimer-B** through a tetranuclear species **T**.

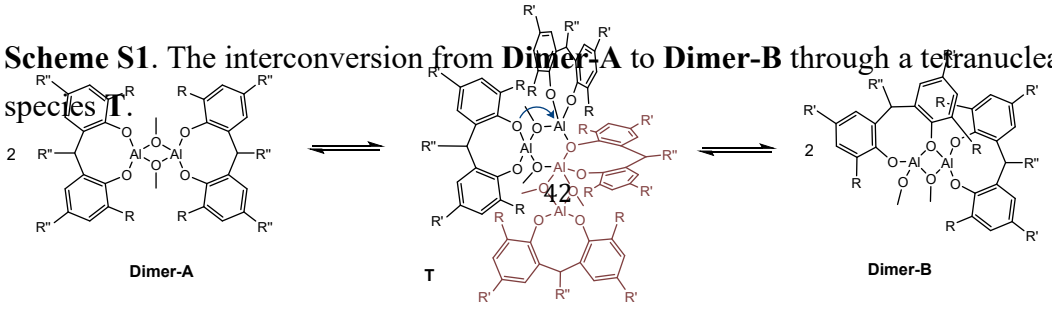

Reference

(1) *Gaussian 09, Revision E.01*; Wallingford, CT, 2009. (accessed.

(2) Liu, Y.-C.; Ko, B.-T.; Huang, B.-H.; Lin, C.-C. Reduction of Aldehydes and Ketones Catalyzed by a Novel Aluminum Alkoxide: Mechanistic Studies of Meerwein−Ponndorf−Verley Reaction. *Organometallics* **2002**, *21* (10), 2066-2069.

(3) Chen, H.-L.; Ko, B.-T.; Huang, B.-H.; Lin, C.-C. Reactions of 2,2‘-Methylenebis(4-chloro-6-isopropyl-3-methylphenol) with Trimethylaluminum: Highly Efficient Catalysts for the Ring-Opening Polymerization of Lactones. *Organometallics* **2001**, *20* (24), 5076-5083.

(4) Taden, I.; Kang, H.-C.; Massa, W.; Spaniol, Thomas P.; Okuda, J. Alcoholysis of Aluminum Alkyls Supported by Bulky Phenoxide Ligands: Synthesis, Characterization, and ϵ-Caprolactone Polymerization Activity of Two Dimeric Aluminum Isopropoxides. *Eur. J. Inorg. Chem.* **2000**, *2000* (3), 441-445.

(5) Ko, B.-T.; Wu, C.-C.; Lin, C.-C. Preparation, Characterization, and Reactions of $[(EDBP)Al(\mu\text{-}O^{i}Pr)]_2$, a Novel Catalyst for MPV Hydrogen Transfer Reactions. *Organometallics* **2000**, *19* (10), 1864-1869.